Conjugated Polymers for Aptasensing Applications

Razieh Salimian, Corinne Nardin

Conjugated Polymers for Aptasensing Applications

Razieh Salimian[a#‡*], *Corinne Nardin*[a‡*]

[a]*Universite de Pau et des Pays de l'Adour, E2S UPPA, CNRS, IPREM, Pau, 64053, France*

*Email: corinne.nardin@univ-pau.fr, rs2964@bath.ac.uk

‡R.S and C.N contributed equally to this paper.

ABSTRACT. Rapid and specific assaying of molecules that report on a pathophysiological condition, environmental pollution, or drug concentration is pivotal for establishing efficient and accurate diagnostic systems. One of the main components required for the construction of these systems is the recognition element (receptor) that can identify target analytes. Oligonucleotide switching structures, or aptamers, have been widely studied as selective receptors that can precisely identify targets in different analyzed matrices with minimal interference from other components, in an antibody-like recognition process. These aptasensors, especially when integrated into sensing platforms, enable a multitude of sensors that can outperform antibody-based sensors in terms of flexibility of the sensing strategy and ease of deployment to areas of limited resources. Research into the compounds that

efficiently enhance signal transduction and provide a suitable platform for conjugating aptamers has gained a huge momentum over the past decade. The multifaceted nature of conjugated polymers (CPs), notably their versatile electrical and optical properties, endows them with a broad range of potential applications in optical, electrical, and electrochemical signal transduction. Despite the substantial body of research demonstrating the enhanced performance of sensing devices using doped or nanostructure-embedded CPs, few reviews are available that specifically describe the use of conjugated polymers in aptasensing. The purpose of this review is to bridge this gap and provide a comprehensive description of a variety of CPs, from a historical viewpoint underpinning their specific characteristics and demonstrating the advances in biosensors associated with the use of these conjugated polymers.

1. INTRODUCTION

Owing to technological advances, current accurate data monitoring in various applications, including pharmaceuticals assessment, environmental testing, forensic science, food analysis, and clinical diagnostics can be easily accomplished using analytical sensing devices. A sensor is usually an electronic device that is composed of (i) a transducer, that recognizes the target analyte and converts this chemical interaction into a measurable signal (e.g., colorimetric, fluorometric, surface plasmon resonance (SPR), conductometric, field-effect transistor (FET), electrochemiluminescence (ECL), photoelectrochemical (PEC) and electrochemical setting), (ii) an electronic circuit for signal processing, and (iii) a showcasing component, to display the output signal. Sensors utilizing biorecognition elements (e.g., aptamers, antibodies, peptides, affimers, nucleic acids, and enzymes) to detect specific targets are referred to as biosensors.[1] In general, a biosensor's function is significantly depending on the affinity of the biorecognition element towards target analyte, the signal transduction, and amplification. Consistent with this, increasing interest is being drawn into incorporating aptamers (in terms of selectivity) and nanomaterials and/or nanocomposites (in terms of detection sensitivity) into sensing platform.[2-4]-Such amplification can effectively boost the biosensor performance.[5-8]

The advent of conjugated polymers, depicted in **Figure 1**, has supported studies in multiple fields including energy storage, design of nanoelectronic and optical devices, and chemical and biological sensors.[9]

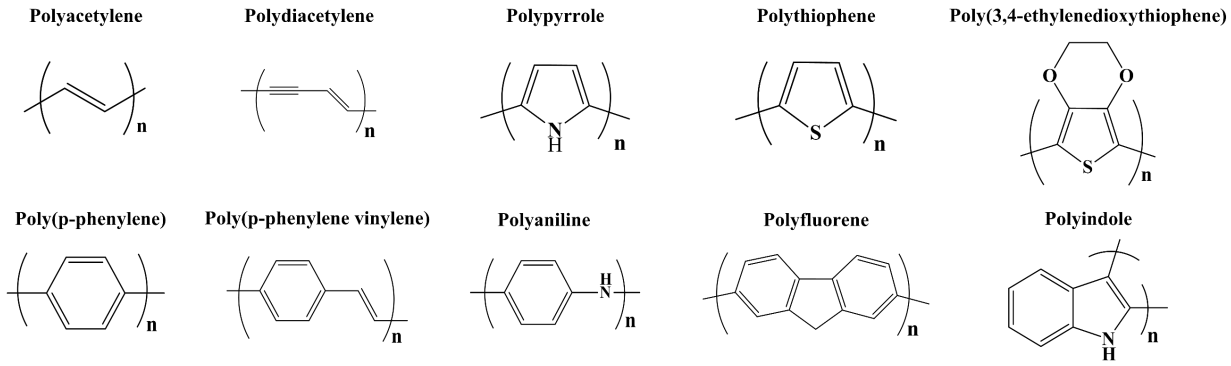

***Figure 1**. Monomeric platforms for multiple conjugated polymers*

CPs are cost-effective materials that are easily processed (on various substrates),via chemical/electrochemical methods and exhibit both electroactive and photoactive properties. In addition, their electrical conductivity, biocompatibility, sensitivity, mechanical and thermal stability make them attractive for biosensor construction.[10, 11] Moreover, their rich synthetic chemistry offers the possibility of fine-tailoring with versatile functional groups for a particular application (e.g., immobilization of biological components, the introduction of redox activity, change of conductivity, modification of optical property, controlling the steric hindrance in the polymer chain, etc.).[12]

From a structural perspective, these π-conjugated polymers possess high electron mobility along the individual chain, commonly referred to as molecular wires. Doping these CP structures to generate positive or negative charge carriers within the polymeric backbone has

been demonstrated to enhance their optical properties and electronic conductivity.[13, 14] Depending on the type of CP, either n-type (electron injection into CP backbone) or p-type (withdrawing electron from CP backbone; i. e. hole injection), doping could raise the polymer's conductivity from insulating to metallic state.[12, 15] **Figure 2** depicts the doping process and how it affects the various properties of CPs. In terms of optical properties, it has been reported that upon doping, transparent CP with a wide band gap turns colored, similarly, a colored CP with a medium band gap becomes transparent when oxidized.[12, 16] **Figure 2B** shows UV-vis reflection spectra of polyaniline (PANI) and UV-vis absorption spectra of poly(3,4-ethylenedioxythiophene) (PEDOT) showcasing the alternation of optical property of the electroactive polymers by an electrochemically induced redox reaction; a phenomenon called electrochromism (Platt., 1961).[17-20] These redox processes modify the electronic properties of the polymer, causing alterations in its color. Oxidation or reduction (doping) of the polymer results in a modification of the band gap (E_g), which is the energy difference between the highest occupied molecular orbital (HOMO) and lowest unoccupied molecular orbital (LUMO) potentials. These modifications in the band gap led to color changes, enabling electrochromic materials to display a range of colors.[21]

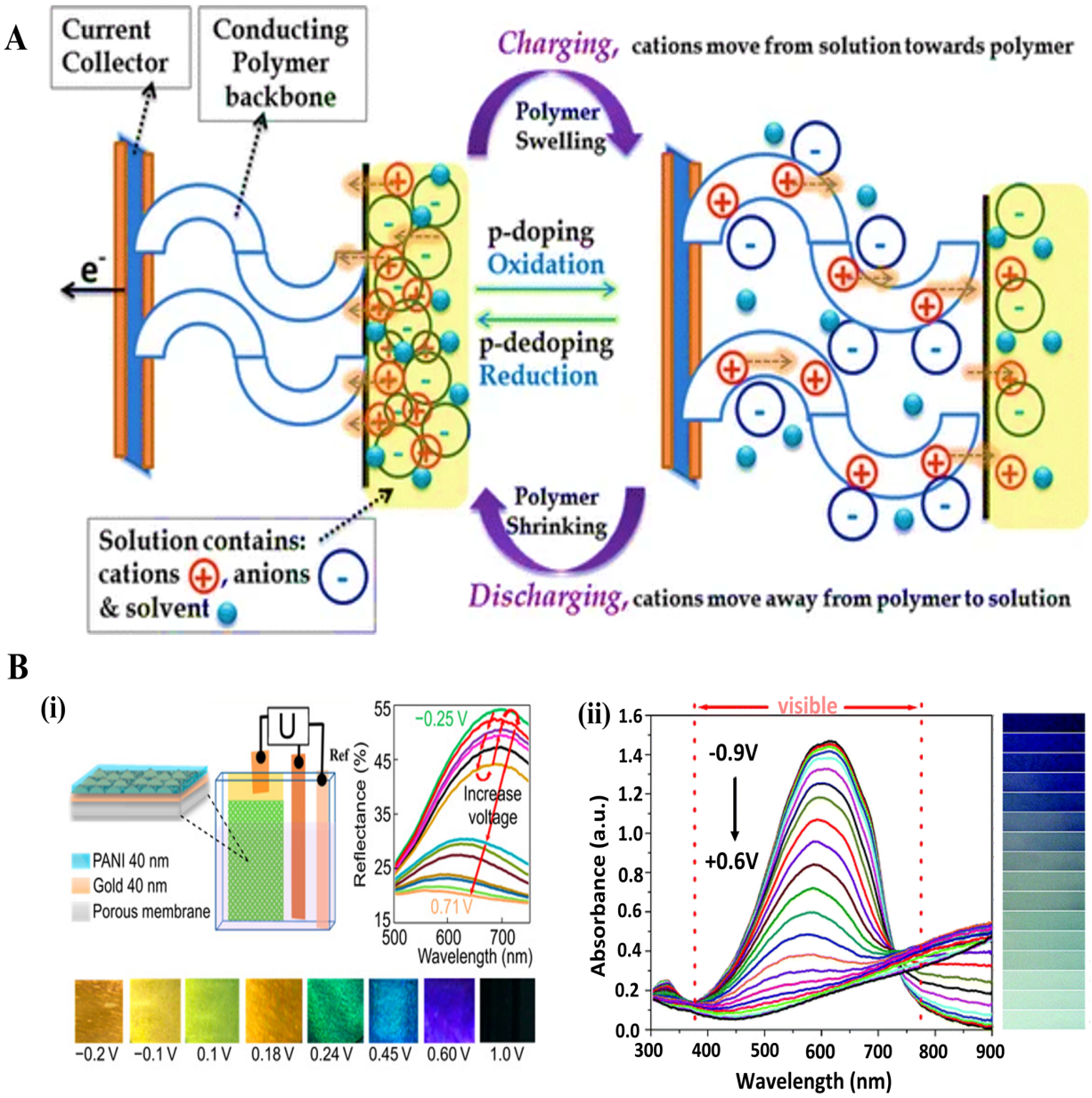

Figure 2. *(A) Diagram illustrating the reversible electrochemical p-doping/p-dedoping of CPs. Adapted with permission from Ref.[15] Copyright© 2016, Springer International Publishing Switzerland. (B) Spectroelectrochemistry of (i) PANI and (ii) PEDOT film: optical variation in the visible region as a function of applied potentials and the respective produced colors, from an electrochromic device. Adapted with permission from Ref.[18] Copyright© 2019 American Chemical Society and from Ref.[20] Copyright© 2005 Royal Society of Chemistry.*

In addition to doping, the incorporation of nanomaterials (e.g., carbon nanostructures and metal nanoparticles; either as dopants or hybrid) in the polymer matrix can also affect the properties of the final polymer composite.[22-24] Accordingly, the increased surface area, high catalytic activity, enhanced charge/electron transport, and improved mechanical stability

(i.e., related to the synergistic effect), contribute to stability, reproducibility, fast response, and low limit of detection (LOD) of the designed sensing device.[25] Despite the remarkable features of these doped molecular wires and their nanohybrid polymeric composites, there is still a need for further improvement in the sensing performance of CP-based devices in terms of selectivity. Molecularly imprinted polymers (MIPs), mimicking biorecognition elements, were introduced as synthetic receptors to address this issue.[26] However, limitations related to imprinting bio-macromolecules (e.g., larger cell and microbial cell), deep template embedding, proteins with similar conformations, and difficult accessibility to binding sites, [27, 28] have led to the search for potentially more promising alternatives.

The huge library of biorecognition elements (e.g., enzymes, affimers, cells, peptides, and nucleic acids) highlights the selectivity in detection methodology. Of special focus, aptamers have gained a huge interest, by virtue of the ease of their synthesis, selection, and production. Nucleic acid aptamers are single-stranded RNA or DNA oligonucleotides that are synthesized by selection from a large random sequence pool, in the process of systematic evolution of ligands by the exponential enrichment (SELEX) process targeting wide range of analytes (e.g., ions, metals, toxins, small molecules, whole cells, bacteria, proteins, and DNAs).[29, 30] Aptamers, known as artificial chemical antibodies, outperform other biological elements in terms of affinity and stability, based on reports.[31-34] Aptamers can be easily immobilized/entrapped on/into the polymer backbone through physical or chemical bonding, where the aptamer-target interaction is translated into various readable signals

including optical, electrochemical, and electrical signal.[30] Integrating aptamers within CPs has supported their sensing capabilities, as a conformational change of the aptamer upon binding to a target is reflected by a change in the intrinsic properties of the CP. Currently, aptamers play a pivotal role in designing electroanalytical devices for different applications, clinical trials, and detection of environmental, and food contamination. (a) detection of mycotoxins (e.g., ochratoxin A (OTA) and aflatoxin B1 (AFB1)) (OTA-Sense and AflaSense; NeoVentures Biotechnology Inc.), (b) detection of active thrombin (OLIGOBIND®Thrombin activity assay, Sekisui diagnostics, LLC), (c) isolation of biomarker positive cell (AptoPrep™ and AptoCyto™, AptSci Inc.), (d) discovery and diagnostics of multiple biomarkers (SOMAscan, SomaLogic Inc.), (e) detection of theophylline (Apta-Beacon™, Aptagen, LLC) and recently, (e) rapid Covid-19 diagnostic test (AptameX™, Achiko AG), are some examples of the commercialized aptamer-based diagnostic products that illustrate how quickly the aptasensing methodologies are developing.[35, 36]Herein, we provide a comprehensive overview of CP-based biosensors with the main focus on aptasensors. The principle of detection methodologies and synthesis routes are not discussed in this review given the extensive literature already available in this field.[37-39] A broad range of CPs, classified according to their structure, and their application in biosensing is discussed; starting from DNA biosensors to aptasensors. Furthermore, the concept of polymer doping and the combination of nanomaterials into polymer composite materials is thoroughly addressed in a variety of biosensor designs and methodologies.

2. A REVIEW OF CONJUGATED POLYMER-BASED APTASENSORS SINCE 2010: FROM DISCOVERY THROUGH STRUCTURAL INVESTIGATION TO BIOSENSING; OPTICAL, ELECTRICAL, AND ELECTROCHEMICAL SENSING TECHNIQUES.

A. ALIPHATIC CONJUGATED POLYMERS

i. Polyacetylene (PA)

Historically, polyacetylene (PA) provided the foundation of research on conducting polymers.[40] The first polymerization of acetylene was reported as early as 1958 by Natta and co-workers (i.e., polymerization of acetylene in hexane using $Et_3Al/Ti(OPr)_4$ (Et= ethyl, Pr=propyl) as a catalyst). The prepared polyacetylene with identical structure to a very long conjugated polyene, has not been accepted widely in the field.[41] For 20 years, PA has raised a great deal of interest, possessing the lowest bandgap among studied parent CPs (band gap energy E_g = 1.5 eV),[42] in the optoelectronic field.[43, 44] By the end of the 1970s, Heeger, MacDiarmid, and Shirakawa discovered that PA's conductivity is increased markedly through halogen doping which is referred to as synthetic metal.[45, 46] In 2000, they have been awarded a Nobel Prize in Chemistry *"for the discovery and development of electrically conductive polymers"*.[47]

PA exists in two isomeric conformations named "*cis*" and "*trans*", with the latter being thermodynamically more stable at room temperature. CPs have a common structure of an alternating pattern of single and double bonds.[48] As the number of carbon atoms in

polyacetylene molecule increases, the number of π-electrons increases, and subsequently, the energy levels of π and π* orbitals split further, insofar as these discrete molecular orbitals merge into two quasi-continuous energy bands. These two bands are equivalent to the valence and conduction bands of inorganic semiconductors, as illustrated in **Figure 3A**.[49]

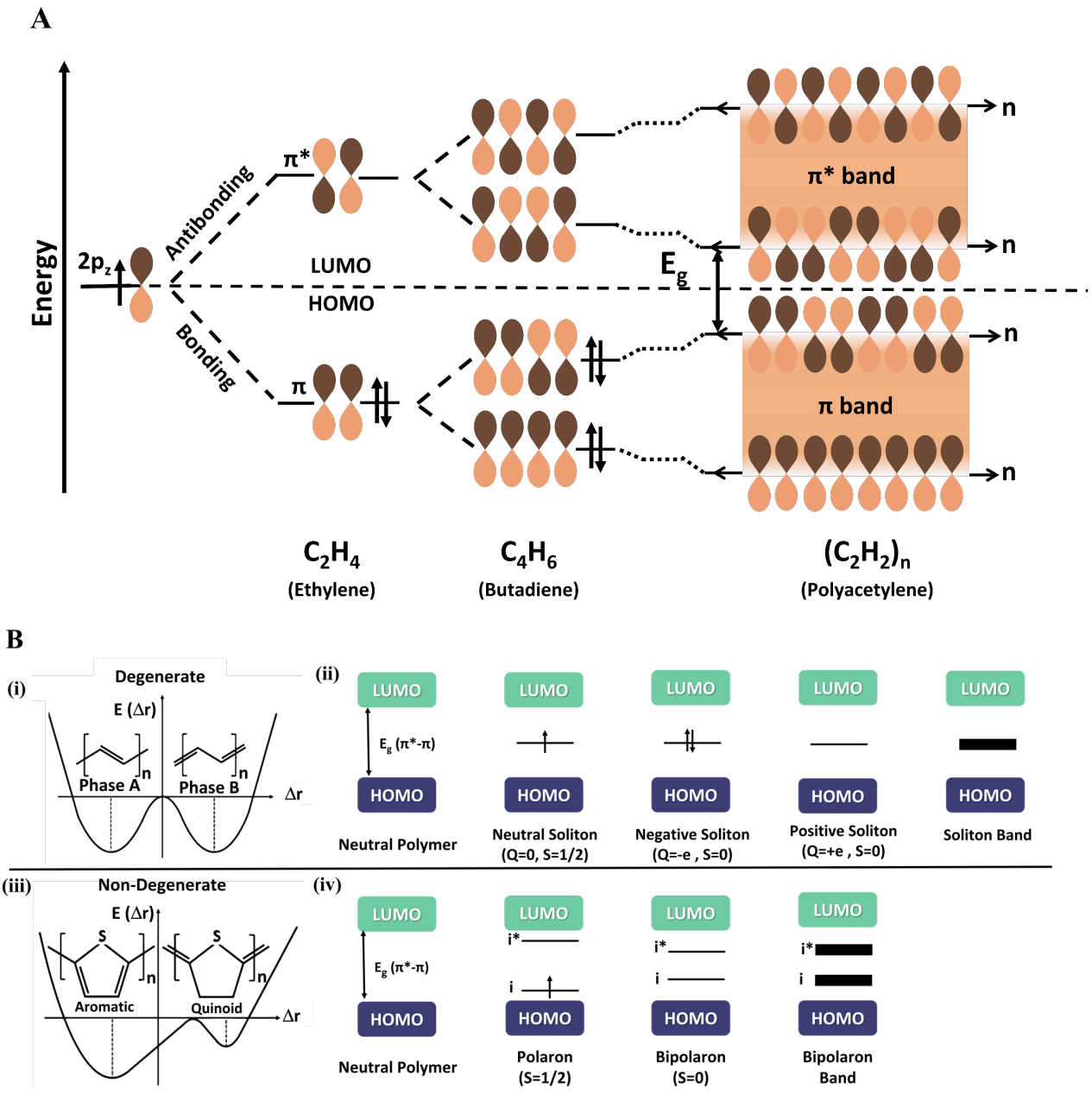

Figure. 3. *Schematic representation of (A) energy diagram for the formation of π orbitals of polyacetylene of various length. (B) (i) and (iii) potential energy change depending on the deformation coordinate of conjugated polymer with the degenerate ground state (trans-polyacetylene (trans-PA)) and non-degenerate ground state (poly(thiophene)), respectively., and (ii) and (iv) the band structure of soliton (e.g., in trans-polyacetylene), and polarons and bipolaron, (e.g., in poly(thiophene)). Adapted with permission under a Creative Commons (CC-BY 4.0) from Ref.*[50] *Copyright © 2020 Elsevier Ltd.*

Two configurations of trans-PA are of identical energy in the ground state (i.e., their occurrence is of equal probability), and they can, thus, coexist in two domains on the same chain, which creates a transition region between the two domains, associated with the

formation of a structural defect known as a neutral soliton.[50] Most π-conjugated polymers, however, have a non-degenerate ground state, and instead, they are composed of aromatic and quinoid structures that are energetically inequivalent (**Figure 3B** ((i) and (iii)).[50, 51] On doping, the self-localized excitations are formed, called quasi-particles including solitons (neutral, positive, and negative soliton), polarons, and bipolarons, that move relatively free along polymer chains.[52] Solitons are the charge carriers in degenerate systems (e.g., trans-polyacetylene), conversely, polarons and bipolarons are the charge carriers in both degenerate and non-degenerate systems (e.g., polypyrrole (PPy), poly(p-phenylene) (PPP), polythiophene (PT)). In trans-polyacetylene, soliton formation creates new electronic states within the band gap.[13, 53] At very high doping levels,[54, 55] these states overlap and broaden to form a soliton band, which eventually merge with the conduction and valence bands, rendering metallic (metallic-like) conductivity to the polymer (**Figure 3B**, (ii)).[47] The electronic bands illustrating the formation of polaron and bipolaron for conjugated polymers with non-degenerate ground state are depicted in **Figure 3B** (iv).

Compared to CPs of larger bandgap categories, this non-aromatic polyene is a less stable polymer, both doped and undoped, being prone to oxidation across the double bond.[56, 57] The interaction of PA with oxygen increases initially, and decreases after a few hours, due to irreversible oxidation which interrupts the flow of charges.[58] To overcome this drawback, substituting the acetylene backbones has been proposed as an alternative to improve the properties of PA. Disubstituted polyacetylenes have been found to have a strong thermal

decomposition resistance and an efficient emission of blue light.[59] Research on PA is mainly focused on developing fluorescent-based chemosensors capable of capturing analytes directly through their functional groups.[60-63] It is worth noting that the discovery of PA prompted studies on the (semi)conducting properties of numerous π-conjugated polymers and further research efforts in the biosensing field.

ii. Polydiacetylene (PDA)

In 1969, Wegner et al. synthesized a new polyacetylene-like compound, resulting from the 1,4-photopolymerization of diacetylene under ultraviolet (UV) irradiation (**Figure 4A**).[64]

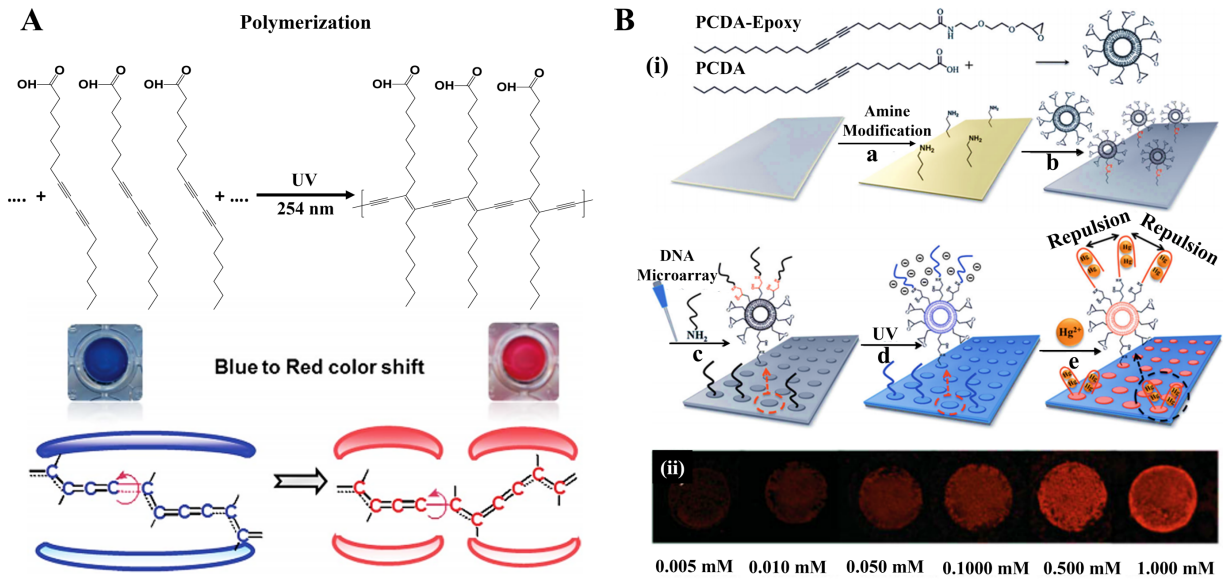

Figure 4. *(A) Polymerization and colorimetric characteristics of PDAs. Adapted with permission from Ref.[65] Copyright© 2013 Royal Society of Chemistry. (B) (i) Schematic illustration of the formation of PDA liposome from diacetylene monomers; PCDA and PCDA-Epoxy. followed by the depiction of a PDA-based microarray for mercury detection. (ii) Fluorescence microscopy images of the PDA liposome arrays after 1 h incubation at room temperature with Hg^{2+} solutions in various concentrations. Adapted with permission from Ref.[66] Copyright © 2009 WILEY-VCH Verlag GmbH & Co. KGaA, Weinheim*

Polydiacetylenes (PDAs) possess remarkable optical properties including a colorimetric transition from blue to red along with fluorescence enhancement triggered by external

stimuli, such as temperature, pH, pressure, and the presence of biological molecules, which makes them promising options for sensing application (**Figure 4A**).[67] Diacetylene monomers can be organized into various self-assembled configurations, (e.g., vesicles, Langmuir–Blodgett monolayers, and single crystals),[65, 68] which impact the physical, thermal, and mechanical properties of the final polymeric structure.[69] Among these structures, amphiphilic vesicles/liposomes (in the form of spherical lipid bilayer structures), are the most commonly used structure of PDAs in sensing methodology.[70]

Detection of biological molecules using PDA structures dates back to 1995 when Charych et al.[71] introduced PDA-vesicles decorated with specific binding ligands for the detection of influenza virus and cholera toxin.[72, 73] A wide range of functional groups can be incorporated into the monomer structure to facilitate the attachment of biorecognition elements, which upon binding to the analyte, impose stress on the polymer backbones, resulting in analyte recognition.[74] One of the first aptamer-conjugated PDA-liposome was reported by Lee et al.[66] In this platform, the sensor exhibits a color change due to the specific binding of aptamers, tethered to the epoxy-terminated 10,12-pentacosadiynoic acid (epoxy-PCDA), to mercury(II) ions. The conjugated ene-yne backbone of PDA-liposomes is perturbed by the steric repulsion force between bulky T-Hg-T complexes (T; Thymine), resulting in red fluorescence emission (LOD = 5 μM) (**Figure 4B**). In another study, Wen et al. used 10,12-tricosadiynoic acid (TCDA) liposomes to examine the sensitivity by incorporating aptamer with different linker lengths, base lengths, and configurations, each having a differing effect

on steric repulsion, for the naked-eye detection of Zn^{2+} (LOD = 125 μM).[75] **Table 1** presents an array of PDA-based aptasensors, mostly using optical methods, designed for the detection of various analyte targets, such as ions, bacteria, and cells.[76-80]

Table 1. Examples of PDA-based aptasensors

Analyte	PDA Liposome	Detection Method	Linear Dynamic Range (LDR)	LOD
Thrombin[76]	TCDA-NHS:PCDA	Colorimetry	0 – 10 μM	0.5 μM Limit of visual detection
E. coli O157: H7[79]	PCDA	Colorimetry	10^4 - 10^8 CFU/mL	10^4 CFU/mL
MUC1 [78]	PCDA-NHS:PCDA	Fluorescence	0–50 nM	0.8 nM
Potassium[77]	PCDA-linker-NHS:PCDA	Colorimetry Fluorescence	- 0.5–50 mM	0.1 mM 0.5 mM
Bacillus thuringiensis[80]	TCDA-NHS:PCDA	Colorimetry	-	3×10^7 CFU/mL (3×10^7 - 3×10^{11} CFU/mL)

In most of these examples, **PCDA** is used as a spacer in liposome structure. Escherichia coli O157: H7 (E. coli).
NHS: n-hydroxysuccinimide

B. AROMATIC AND HETEROAROMATIC CONJUGATED POLYMERS

i. Polyaniline (PANI) and PANI derivatives

Polyaniline (PANI) has a longer history than polyacetylene, which started with Ferdinand Runge's report on aniline oxidation in 1834 and was completed by Henry Letheby's report on its electrochemical oxidation in acidic media in 1862.[81] In the early stages, aniline black was considered as an aniline octamer in different oxidation states.[82] Afterward in 1910, Green and Woodhead described different oxidation states ranging from the fully reduced leucoemeraldine through the partially oxidized protoemeraldine, emeraldine and nigraniline, to the fully oxidized pernigraniline.[83] However, PANI was not called polymers for a long

time, since the existence of macromolecules was not accepted until the 1920s.[84] In 1967, the first real breakthrough for PANI came with Rene Buvet and Marcel Jozefowicz, who proposed that this organic protolytic poly-conjugated macromolecule has redox properties and its conductivity is of electronic origin. Additionally, they demonstrated that PANI possesses ion-exchange properties.[85] Afterward, Diaz and Logan conducted further studies on the formation of the electroactive polyaniline films based on their initial research on pyrrole electropolymerization.[86] Studies on PANI showed that the conductivity of PANI depends on two main variables: the oxidation state of the polymer and the degree of protonation of the nitrogen atoms within its backbone and can be controlled reversibly by doping mechanisms (**Figure 5**).[82, 87-91] It has been established that the protonated emeraldine form of polyaniline is the most conductive.[92]

A **Basic Structure of PANI**

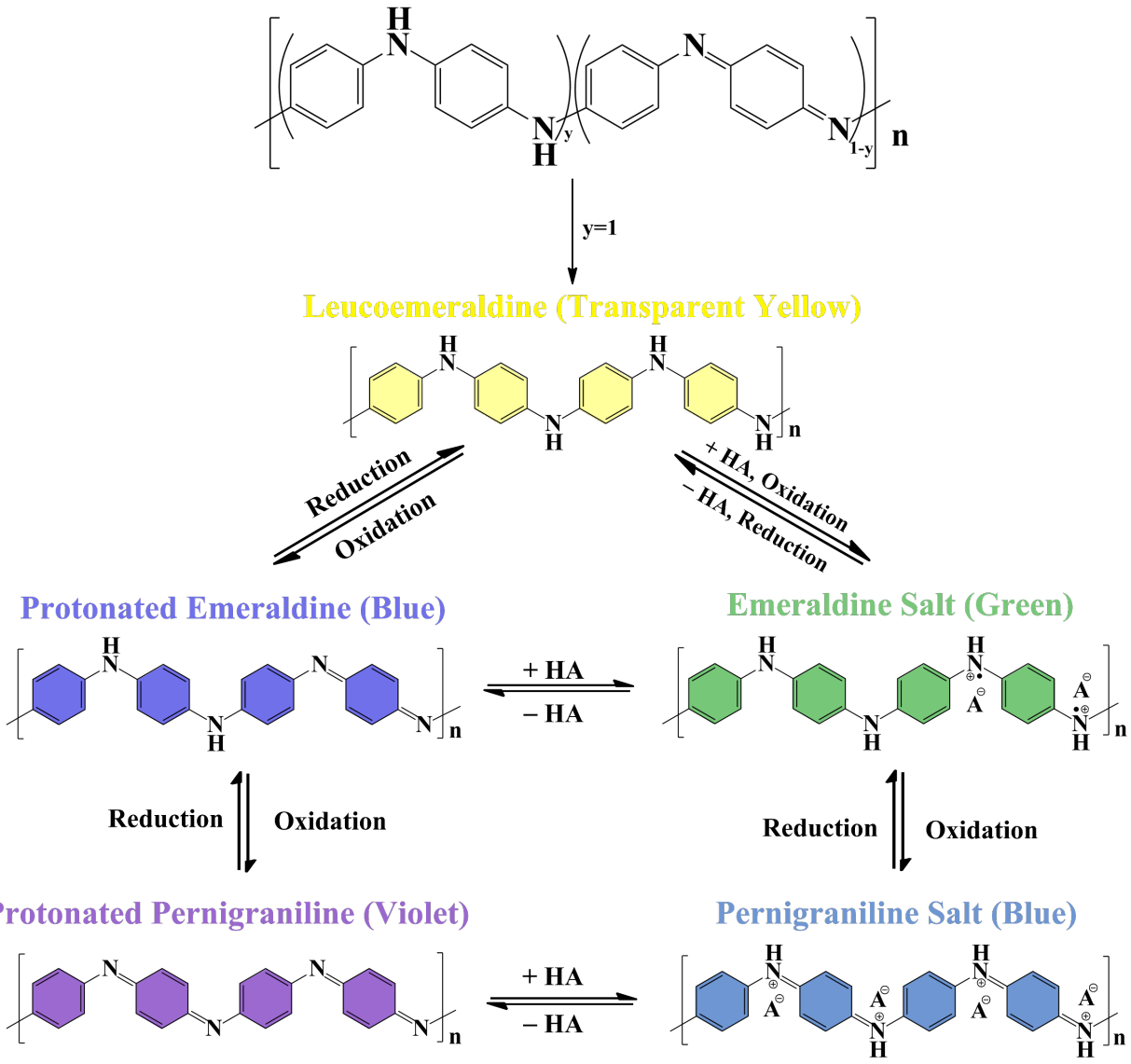

B

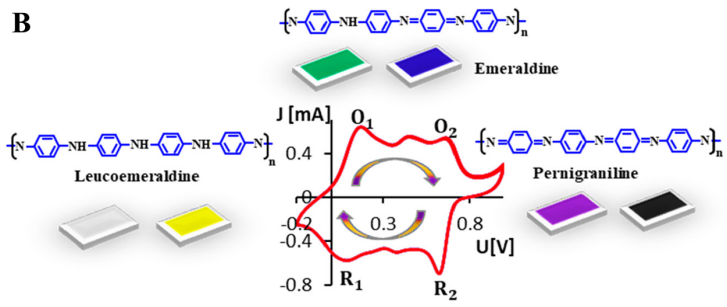

***Figure 5**. (A) Different redox/protonation states of PANI and their corresponding colors. Adapted with permission under a Creative Commons (CC-BY 4.0) from Ref.[90]. Copyright © 2017 MDPI. (B) Another view of PANI states and color switching during cyclic voltammetry experiment. Adapted with permission from Ref.[18]. Copyright© 2019 American Chemical Society.*

The first PANI-based DNA hybridization assay was developed using gold nanoparticles-doped PANI (i.e., in neutral media), and analyzed using both electrochemical (EC) and surface plasmon-enhanced fluorescence spectroscopy (SPFS) methods.[93] Thereafter, Luo and coworkers reported the first label-free conductometric aptasensor for the detection of immunoglobin (IgE) in 2011.[94] In general, PANI-based sensors offer a valuable advantage in biosensor design due to their amino-rich surface, which facilitates the attachment of biomolecules. In this work, upon the target-aptamer binding, the conductance of electrochemically synthesized PANI nanowires rapidly increases due to the accumulation of negatively charged IgE (in pH 7.4 PBS, pI=5.2-5.8) in a p-type nanowire which resulted in a fast and real-time sensing assay accompanied by excellent specificity and ultra-sensitivity (LOD=0.56 pg mL^{-1} which corresponds to a 2.8 fM concentration, in 5s).

The development of PANI-based nanocomposites is an effective method for incorporating new features into polymer materials and enhancing their properties.[95, 96] Taking this into account, Liu et al. studied the graphene/PANI-based aptasensor for the sensitive detection of dopamine using square wave voltammetry (SWV). Upon introduction of the target, binding-induced steric hindrance reduces the efficiency of electron transfer of the $Fe(CN)_6^{3-/4}$ redox probe, leading to the decrease of the electrochemical current. The aptasensor demonstrated a limit of detection as low as 0.00198 nM.[97]

PANI exhibits an intriguing reversible redox behavior, making it a suitable option for (bio)electrochemical sensing applications as its signal can be triggered by external stimuli. However, the redox activity of PANI ceases in aqueous media at pH > 4, thus restricting its application to specific bioassays. To overcome this drawback, adding self-doping functional groups to the polymer backbone,[98] doping PANI with negatively charged structures (e.g., polyelectrolytes[99], metal[100], and carbon nanostructures[101]) were proposed as alternative strategies to extend its electroactivity beyond neutral pH. Generally, the inserted groups (e.g., sulfo, carboxyl) change the micro-environment of the nitrogen atoms in the PANI chain and shift the local pH.[102] Accordingly, Su. et.al. designed a thrombin detection platform based on self-doped PANI, fabricated chemically in the presence of multiwalled carbon nanotubes (MWCNTs), by following the redox signal of PANI-MWCNTs in phosphate buffer solution (pH 7.4), (LOD of 80 fM).[103]

Besides serving as the electrode modifying layer, the application of PANI as an electroactive probe was also investigated for bioanalyses. This approach involved the deployment of CPs, alone or in the form of polymeric nanocomposite, decorated with secondary biorecognition elements (e.g., antibodies and nucleic acids; also known as nano-bioconjugates),[104] to enhance signal transduction and highlight the presence of target.[105] The role of labels in the signal amplification pathway is categorized as follows: (i) catalyst, (ii) redox-active species, or (iii) carrier of reporter molecules.[106] Therefore, polymers having specific properties could act as redox tags, carry redox probes, or exhibit catalytic activity,

enabling the sensing signals to be further enhanced. For instance, in the aptasensor developed by Bai et al., the excellent redox and electrocatalytic activity of the fullerene-doped PANI (C_{60}-PANI) nanohybrids applied for highly sensitive detection of the mycobacterium tuberculosis MPT64 antigen. The MPT64 antigen was detected in the range of 0.02 to 1000 pg mL^{-1} by differential pulse voltammetry (DPV) (**Figure 6A**).[107]

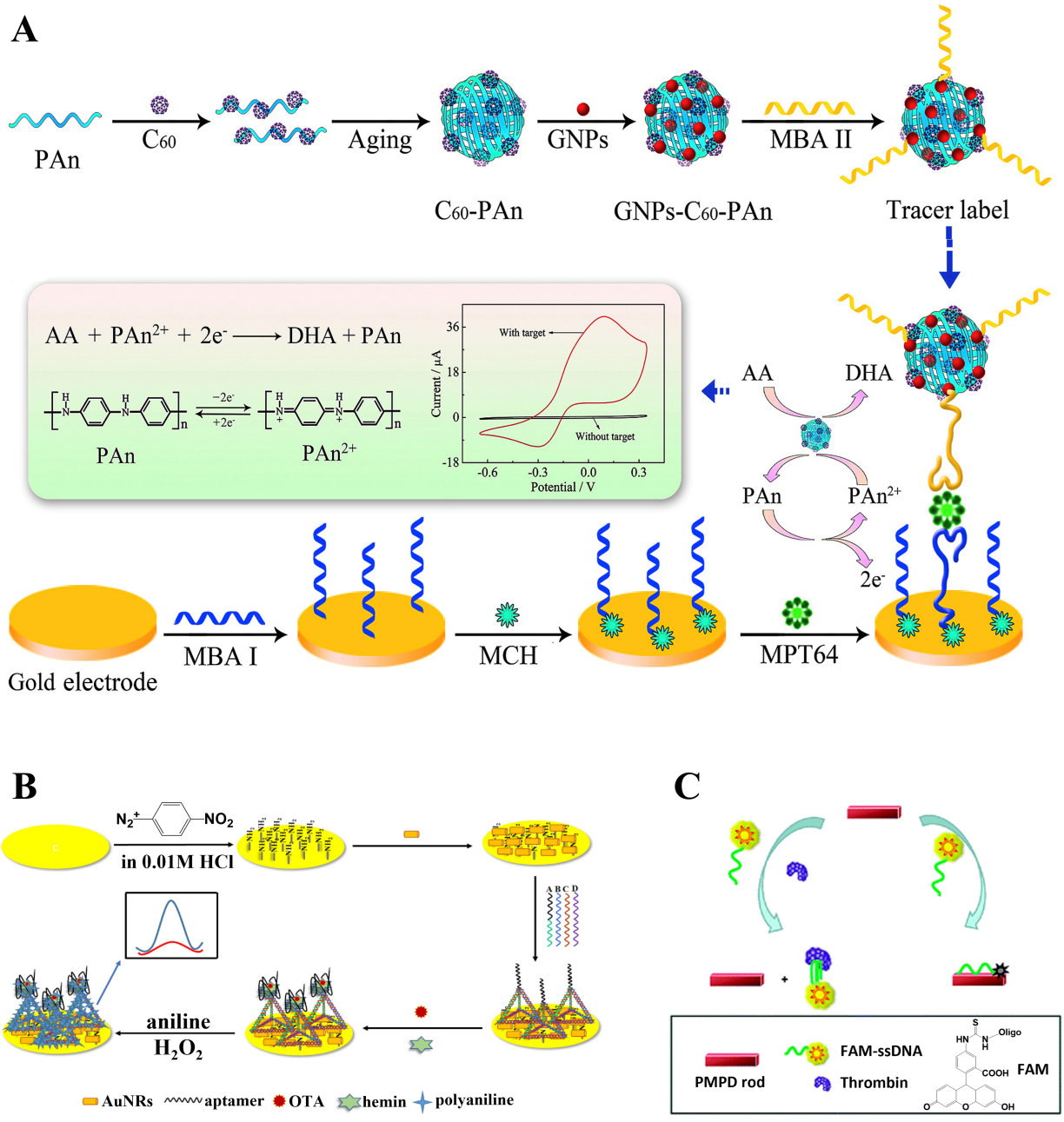

Figure. 6. *Schematic diagram to illustrate (A) the preparation of PANI-based tracer label and the signal amplification mechanism for MPT64 detection. Adapted with permission from Ref.*[107]*. Copyright © 2017 Elsevier Ltd. (B) hemin/G-quadruplex/DNA tetrahedral nanostructure/Au nanorods/NH_2-AuE sensor for OTA detection. Adapted with permission from Ref.*[108]*. Copyright © 2018 Elsevier B.V. (C) thrombin detection mechanism using a PMPDA rod-based fluorescent aptasensor. Adapted with permission from Ref.*[109]*. Copyright 2011, Royal Society Chemical.*

In another study, Wei et al.[108] described the use of a hemin/G-quadruplex structure, as HRP-mimicking DNAzyme, for ochratoxin A (OTA) detection. They described that the formation of hemin/G-quadruplex in the presence of OTA catalyzes the oxidation

polymerization of aniline to PANI in the presence of H_2O_2, on DNA tetrahedral nanostructures (DTN) as depicted in **Figure 6B**. The amplified signal of PANI was recorded in the acetate buffer (pH 4.3). The reported procedure showed a wide linear detection range spanning two orders of magnitude, with a detection limit as low as 0.26 pg mL^{-1}.

Other than electrochemical techniques, PANI has also been applied in electrochemiluminescence (ECL) bioassays, which involve the emission of light from electrochemical reactions. In the development of an ECL cytosensor, electrochemical approaches were used for in situ synthesis of NiS@CdS/PANI nanofibers to detect MCF-7 cancer cells. The amplified ECL emission was monitored in PBS containing $K_2S_2O_8$ (pH 7.4), as a co-reactant, in a wide linear dynamic range of concentration from 12 to 1.2×10^6 cells mL^{-1}, with a limit of detection as low as 8 cells mL^{-1}.[110]

Following the development of aptasensors based on PANI, phenylenediamine (PDA), and aminobenzoic (ABA) acids, other derivatives of aniline with distinct properties from aniline itself, were also considered. Although the conductivity of these redox-active polymers is lower than that of the parent PANI, the outstanding properties of these functional polymers have stimulated increased interest owing to their homogeneous electrochemical deposition and strong adherence to solid surfaces.[111] Moreover, carboxylated polyanilines, known as self-doping structures, possess a high electron density of carboxyl groups and a high biomolecule binding capacity. These features render polyaniline derivatives suitable candidates for both optical and electrochemical biosensing.[112] The first fluorescent aptasensor

for thrombin detection using polymethylphenylenediamine (PMPDA) rods as a sensing platform was introduced by Zhang and coworkers.[109] Since PMPDA reveals no absorption in the visible range, they believed that the photoinduced electron transfer (PET) from a nitrogen atom of PMPDA to an excited fluorophore FAM-labeled aptamer, adsorbed *via* π–π stacking on the PMPDA surface, caused quenching of the dye fluorescence that is regenerated in the presence of the target protein. This mechanism was utilized for sensitive detection of thrombin (LOD=100 pM) which is much lower than that of commonly reported for carbon nanostructures (**Figure 6C**). **Table 2** summarizes the biosensing applications of PANI and PANI derivatives in a variety of buffered media toward the detection of arrays of analytes mainly through electrochemical methods.[113-138]

Table 2. PANI-based Aptasensors

Analyte	PANI and/or its derivatives	Detection Method	Reporter Species/Signal Reporter	LDR	LOD
OTA[126]	ITO/PANI	EIS	$Fe(CN)_6^{3-/4-}$	0.1 ng/mL^{-1} – 10 ng mL^{-1} 1 µg/mL^{-1} – 25µg mL^{-1}	0.1 ng mL^{-1}
Thrombin[113]	GCE/AuNPs/MPTS-GOD/Au-PANI-Graphene	CV	$FAD/FADH_2$ (redox couple of GOD)	1.0×10^{-12}-3.0×10^{-8} M	5.6×10^{-13} M
Kanamycin[138]	GCE/PANI-Graphene/PAMAM–Au NPs	DPV	HQ	5×10^{-6} - 4×10^{-2} µg mL^{-1}	4.6×10^{-6} µg mL^{-1}
Oxytetracycline (OTC)[137]	GCE/GO-PANI/Au NPs	CV	HQ	4.0×10^{-6}- 1.0 mg L^{-1}	2.3×10^{-6} mg L^{-1}
Tetrodotoxin (TTX)[116]	GCE/PANI/PSSA	EIS	PANI ABS (pH 4.8)	0.23–1.07 ng·mL^{-1}	0.199 ng mL^{-1}
Acetamiprid[127]	SPE/PANI/Au NPs	DPV	1-naphthol		0.086 µM

Cocaine[119]	SPE/3D-MRGO/PANI/AuNP	EIS	$Fe(CN)_6^{3-/4-}$	0.09 - 85 nM	0.029 nM
E. coli O157:H7[129]	GCE/PANI/Copper-based MOF	DPV	Methylene Blue	2.1×10^1 - 2.1×10^7 CFU mL^{-1}	2 CFU mL^{-1}
Aflatoxin B_1 (AFB_1)[118]	GCE/rGO/MoS_2/PANI@Chitosan@AuNPs	DPV	$Fe(CN)_6^{3-/4-}$	0.01 - 1.0 fg mL^{-1}	0.002 fg mL^{-1}
Thrombin[133]	GCE/PANI/P(3-ABA) inserted in PVA (Hydrogel with Antifouling Performance)	DPV	PANI PBS (pH 7.4)	1 pM – 10 nM	0.64 pM
Zearalenone (ZEN)[120]	GCE/Au NPs-PANI-Au NPs	Amperometry	H_2O_2	1 fg mL^{-1} – 100 ng mL^{-1}	0.45 fg mL^{-1}
Prostate Specific Antigen (PSA)[124]	GCE/PANI/Au NPs (Peptide; Antifouling)	DPV	$Fe(CN)_6^{3-/4-}$	0.1 pg mL^{-1} - 100 ng mL^{-1}	0.085 pg mL^{-1}
Aflatoxin M1 (AFM1)[121]	GCE/Layer-by-Layer PANI (Aptamer within two PANI layers)	CV EIS	PANI PBS (pH 3.0) $Fe(CN)_6^{3-/4-}$	3 to 90 ng mL^{-1}	1-5 ng mL^{-1}
MCF-7 (Human Breast Cancer Cells)[125]	PANI (Branched peptide; Antifouling)	DPV	PANI PBS (pH 7.4)	50 - 10^6 cells mL^{-1}	20 cells mL^{-1}
Dam MTase Activity[123]	ITO/PANI/Au/Peptide (peptide ; Antifouling)	ECL	$ECL_{PTC\text{-}NH_2}$ / $ECL_{Au@luminol}$ (ratiometric signal)	0.05–100 U mL^{-1}	0.02 U mL^{-1}
Staphylococcus aureus (S. aureus)[117]	Sulfonated PANI	EIS	$Fe(CN)_6^{3-/4-}$	1×10^1 – 1×10^5 CFU mL^{-1}	2 CFU mL^{-1}
ATP[135]	GCE/Graphene/PoPD	DPV	Methylene Blue (i.e., labeled aptamer)	10 nM–2 mM	0.3 nM
MUC1[114]	GE/PoPD/AuNPs	DPV	Thionine	1–100 nM	1 pM
Insulin[115]	PGE/PoPD/AuNPs	EIS	$Fe(CN)_6^{3-/4-}$	1.0–1000 nM	0.27 nM
Thrombin[134]	GCE/Au NPs	DPV	PoPD (Nanoprobe) ABS (pH 4.5)	100 fM–20 nM	20 fM
Aflatoxin B_1[128]	SPE/PANI-PAA Copolymer	DPV	1-naphthol		0.086 ng mL^{-1}
β-lactoglobulin[122]	SPE/PANI-PAA Copolymer	DPV	1-naphthol		0.053 μg L^{-1}
Thrombin[136]	GCE/P(p-ABA)	CV	p-aminophenol	0.001 - 1000 ng mL^{-1}	0.3 pg mL^{-1} (8.3 fM)
MUC1[130]	SPE/P(o-ABA)	CV DPV	Methylene Blue	3–10 ppb 1–12 ppb	2.4 ppb 0.62 ppb

IL-6[131]	GCE/P(p-ABA)/p-aminothiophenol/Au NPs	EIS	$Fe(CN)_6^{3-/4-}$	5 pg mL^{-1}–100 ng mL^{-1}	1.6 pg mL^{-1}
IgE[132]	GCE/P(m-ABA) (Peptide-Antifouling)	DPV	$Fe(CN)_6^{3-/4-}$	0.001–50.0 ng mL^{-1}	0.52 pg mL^{-1}

MTPS; 3-mercaptopropyl) trimethoxy silane. **GOD;** Glucose oxidase. **GO;** Graphene Oxide. **PSSA;** poly(4-styrenesolfonic acid). **ABS;** Acetic Buffer Solution. **DEA;** Diethanolamine Buffer. **MOF;** Metal-Organic Framework. 3-**ABA;** 3-aminophenylboronic acid. **PVA;** polyvinyl alcohol. **3D-MRGO;** Three-dimensional magnetic reduced graphene oxide. **MCF-7;** Michigan Cancer Foundation-7. **PTC-NH₂;** The amino-terminated perylene derivative. **PoPD;** Poly(o-phenylenediamine). **PGE;** Pencil Graphite Electrode. **PAA;** Anthranilic acid. **SPE;** Screen-Printed Electrode. **IL6;** Interleukin-6.

Recently, the electrochromic characteristic of PANI has also been studied for the detection of bacteria (*E. coli*) using immunosensors,[139] the approach that has yet to see the use of aptasensing.

ii. Polypyrrole (PPy) and PPy derivatives

In contrast to PANI's long history, one can trace poly(heterocycle)'s roots back to 1915 with work on a black precipitate named "pyrrole black" by Angelo Angeli. Donald Weiss started reproducing the pyrrole 'graphite' synthesis, reported by Riccardo Ciusa, to study its structure and relative conductivity and finally, described it as follows *"……it is assumed that the conductivity is of electronic origin.*". This was nearly 16 years before the report of Diaz and coworkers in 1979 on the synthesis of conductive a polypyrrole film *via* electropolymerization.[140] In addition to describing the optimization of the electro-polymerization process in terms of quality and reproducibility, Diaz also demonstrated that this could be broadened to a wide family of conjugate systems.[141] **Figure 7** depicts the energy diagram and structure of PPy in different doping states.[142]

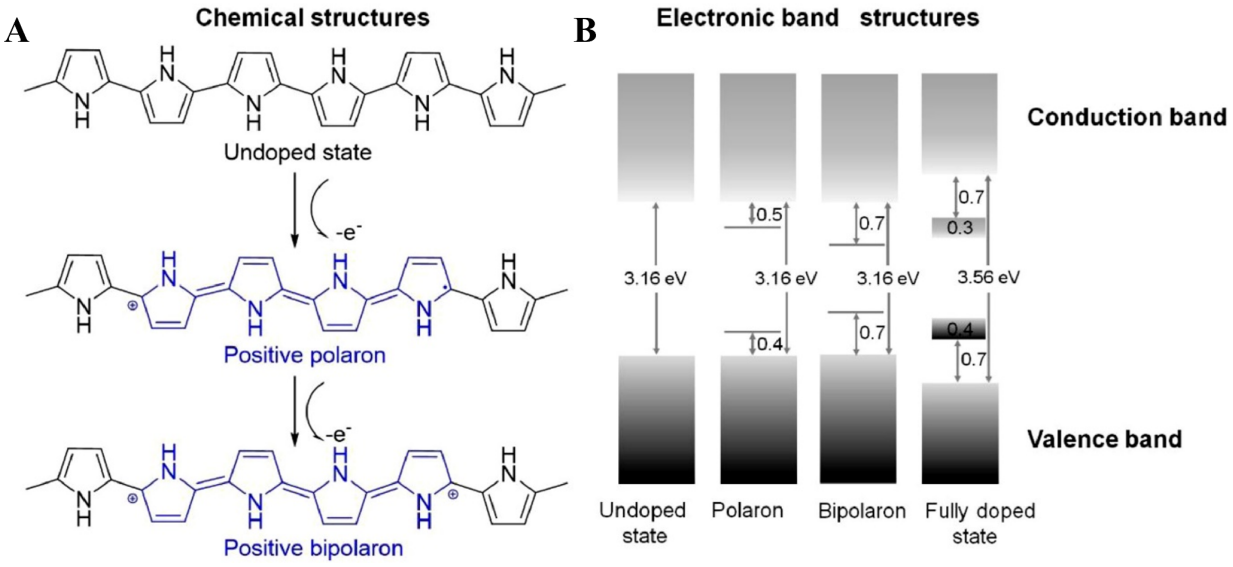

Figure. *7. (A) Chemical and (B) Electronic band structures of PPy in different doping states. Adapted with permission from Ref.*[142]*. Copyright© © 2021 Elsevier Ltd.*

The oxidation potential of PPy (0.8V) is lower than that of any other aromatic heterocyclic monomer, and its polymer is easily synthesized from a range of aqueous and non-aqueous solvents.[143] An oxidation of PPy over this potential (0.8 V) leads to undesirable degradation and loss of electroactivity due to the ejection of dopant. Nevertheless, overoxidation causes the creation of oxygen-containing groups such as carbonyl on the polymer backbone, increasing surface porosity and resulting in improved interaction between the surface and cationic species.[144, 145]

As mentioned earlier, the amine functional groups of PANI are utilized for the covalent attachment of biomolecules onto its scaffolds, whereas in the case of PPy, its derivatives pave the way for assembling bio-elements and designing biosensors, especially in electrochemical sensing platforms. Since the polymerization of aromatic heterocycles is performed through head-to-head coupling (HH, 2-2'), head-to-tail coupling (HT, 2-5'), and tail-to-tail coupling

(TT, 5-5'), 1, 3 and 4-positions are the best positions for the substitution, although, the substitution of monomers results in polymers with reduced electrical conductivity due to steric crowding induced by substituents that twist the polymer backbone from planarity.[146]

The early-stage investigation on DNA recognition using a PPy platform was introduced by Korri-Youssoufi and Garnier in 1997.[147] In this approach, a precursor unit of [(3-acetic acid pyrrole):(3-N-hydroxyphthalimide pyrrole), with low steric hindrance between monomer units, was electropolymerized on an electrode surface which further, was successfully used for the detection of DNA hybridization in an aqueous solution. Afterward, in 2008, Yoon[148] reported PPy-based aptasensors based on FET platform. They depicted a FET sensor decorated with one-dimensional (1D) carboxylic-acid-functionalized polypyrrole (CPPy) nanotubes (CPNT) (copolymer of pyrrole and pyrrole-3-carboxylic acid (P3CA)). Label-free detection of thrombin (LOD= 50 nM) was performed by using an electrolyte as a liquid-ion gate. In this approach, the recognition ability of thrombin aptamers combined with the inherent charge transport property of CPPy nanotubes yielded a direct and label-free electrical readout system. In line with FET-based PPy sensors,[149-157] Kwon. et al.[158] developed a flexible FET-type biosensor based on CPNTs for sensitive detection of vascular endothelial growth factor (VEGF) at limits of detection as low as 400 fM (**Figure 8A**).

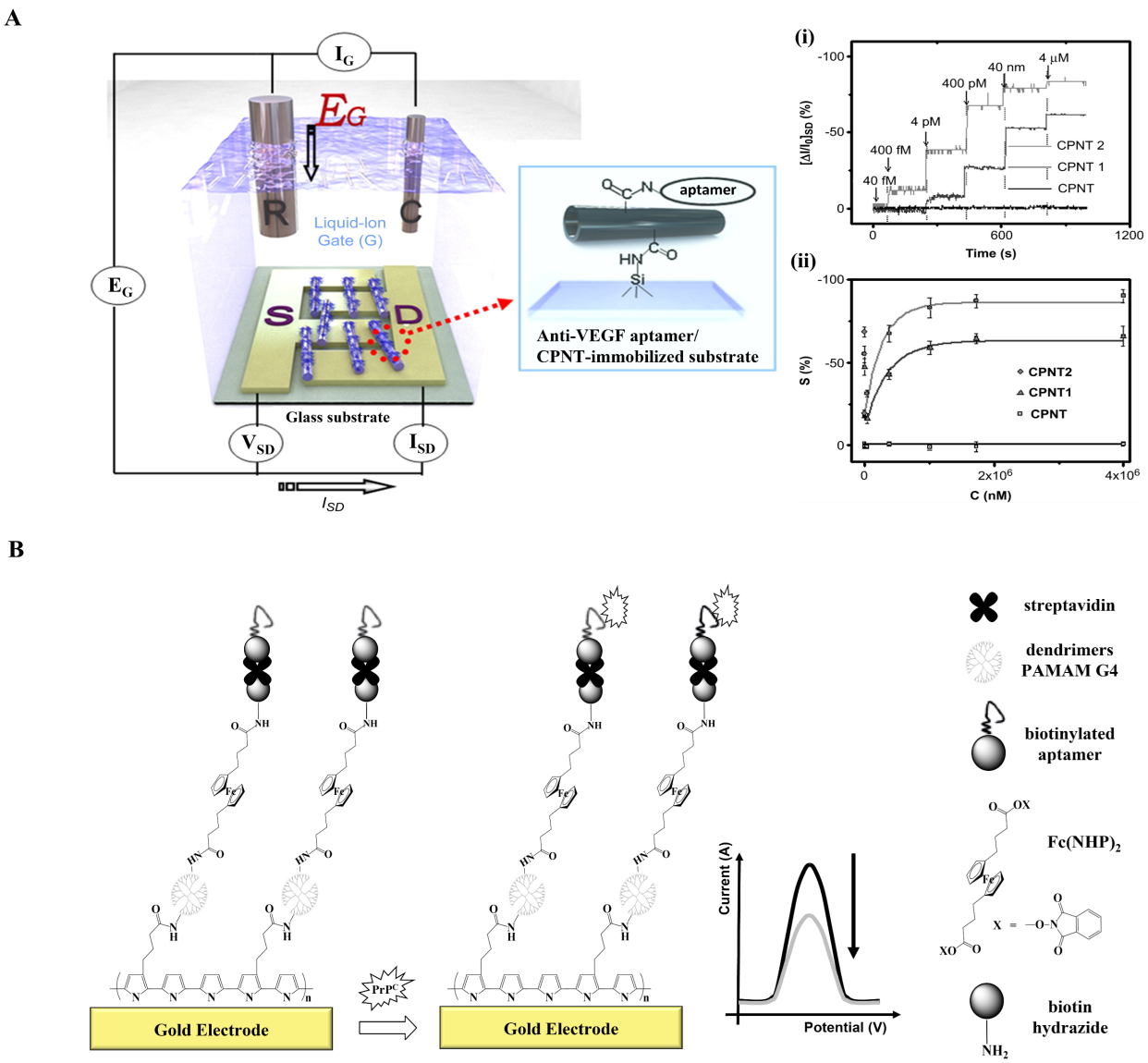
A
I_G
EG
R
C
Liquid-Ion Gate (G)
E_G
S
D
Glass substrate
V_SD
I_SD
I_SD
aptamer
Anti-VEGF aptamer/
CPNT-immobilized substrate
(i)
-100
-50
0
[ΔI/I0]SD (%)
40 nm
4 μM
400 pM
4 pM
400 fM
40 fM
CPNT 2
CPNT 1
CPNT
0
600
1200
Time (s)
(ii)
-100
-50
0
S (%)
CPNT2
CPNT1
CPNT
0
2x10^6
4x10^6
C (nM)
B
Gold Electrode
PrP^C
Gold Electrode
Current (A)
Potential (V)
streptavidin
dendrimers
PAMAM G4
biotinylated
aptamer
Fc(NHP)2
X = —O—N
biotin
hydrazide
NH2
C
(i)
Electrochemical
Deposition
HAuCl4
Electrochemical
Polymerization
ITO
Photocurrent μA
ON
Time (s)
Photocurrent μA
OFF
Time (s)
5FIn
GO
Aptamer
AFB1
(ii)
light
erGO
LUMO
e-
e-
O2
P5FIn
hv
2.51 eV
h+
HOMO
Au
O2-
e-
ITO

***Figure 8**. Schematic representation of (A) the CPNT-aptamer FET-type sensor configuration (R: reference electrode, C: counter electrode, S: source and D: drain, G: liquid-ion gate, EG: gate potential). The FET sensor consists of a three electrodes system that was immersed in an electrolyte (e.g., buffer solution) as a liquid-ion gate. (i) real-time response and (ii) calibration curves of FET sensors toward various concentrations of VEGFs (CPNTi; corresponding to two different diameters of CPNT) Adapted with permission from Ref.[158]. Copyright © 2010 Elsevier Ltd. (B) a biosensor designed for PrP^C detection tracing ferrocene redox signal. Adapted with permission from Ref.[159]. Copyright © 2014 Elsevier B.V. (C) (i) the fabrication process of PEC aptasensor modified with erGO/P5FIn/Au for AFB1 detection and (ii) its corresponding photocurrent generation mechanism of erGO/P5FIn/Au modified electrode. Adapted with permission from Ref.[160]. Copyright© 2019 Elsevier B.V.*

VEGF binding-induced structural switch of the aptamer conformation is triggered as positively charged VEGF molecules (pI=8.5, in pH=7.5) screen out the negative charges of the aptamer. Accordingly, VEGF-aptamer binding can induce positive point charges in the liquid-ion gate dielectric near the CPNTs, leading to the accumulation of negative charge carriers on the CPNTs surfaces and therefore, reducing the p-doping effect in it, which is contributing to the decrease in I_{SD} (i.e., source-to-drain current) by increasing VEGF concentration. To improve sensitivity and increase the loading capacity of the modifying layer, Korri-Youssoufi's group developed a platform composed of redox-sensitive dendrimers combined with PPy for human cellular prions (PrP^C) detection.[159] Using polyamidoamine (PAMAM), as a biocompatible synthetic polymer, allows the conjugation of various molecules owing to its surface functionality. In this approach, pyrrole and 3-(N-hydroxyphthalimidyl ester) pyrrole (PyNHP) were grown as a copolymer on a gold electrode and decorated with PAMAM dendrimers via covalent binding, followed by the attachment of Fc redox markers that act as bridges between specific PrP^C aptamer and PPy. The capture of prion targets triggers a reduction in the Fc signal, attributed to low electron transfer or to slow diffusion of electrolyte to the surface. The sensor was able to detect PrP^C down to 0.8 pM (~1.2 pg mL^{-1}) limit of detection (**Figure 8B**).

Several other approaches were also studied on polypyrrole-based biosensors. For example, Liao et al.[161] constructed a label-free impedimetric sensor based on aptamer-doped PPy. Real-time monitoring of the impedance modulus showed that the sensitivity of the sensor improved from 1 μg mL^{-1} (without polymer) to 10 ng mL^{-1} (with polymer) for specific protein targeting. In another report, Ensafi et al. introduced a platform based on the combination of a molecularly imprinted polymer (MIP) for the detection of bisphenol A (BPA).[156] In this work, PPy was electropolymerized on the pre-immobilized aptamer-BPA complex on the electrode surface, after which BPA was extracted from the MIP structure. Using EIS, this simple strategy enabled a detection limit as low as 0.08 fM and a linear dynamic range of up to 5 pM.[162]

Furthermore, the application of N-substituted PPy have also been reported in sensing platforms. Using electrochemical methodologies, a label-free impedimetric aptasensor based on N-substituted PPy was developed for thrombin detection. Histidine-tagged aptamer was first immobilized on the surface of poly(pyrrole-nitrilotriacetic acid)/Cu^{2+} ((P(py-NTA)/Cu^{2+}). Thrombin recruitment on the such interface was quantified through the EIS perturbations of hydroquinone (HQ), as a redox probe, with LOD of 4.4 pM,~1.2 pg mL^{-1}.[163]

In optical detection mode, the use of PPy was explored for the detection of adenosine based on the fluorescence quenching technique. PPy, as an acceptor, enables the quenching of a wide variety of fluorophores through π-π interaction and plays a critical role in designing optical platform. In this signal-on method, the long-range surface energy transfer

(SET) (i.e., when the donor-acceptor distance > 10 nm) explains the fluorescence quenching of quantum-dots (QDs)-labeled aptamers by PPy, which is restored by the replacement of PPy with adenosine, in proportion to the adenosine concentration (LOD of 10 nM in diluted urine samples).[164] An overview of PPy-based aptasensors is presented in **Table 3**.[149, 151-156, 165-177]

Table 3. PPy-based Aptasensors

Analyte	PPy and its derivatives Structure	Detection Method	Reporter Species/Signal Reporter	LDR	LOD
PDGF-BB[149]	G-IDA/CPMCNF	FET	*	$5 \times 10^0 – 5 \times 10^4$ fM	5 fM
PDGF-BB[151]	Ag patterened electrode/Graphene/$Co(OH)_2$@CPPy	FET	*	1.78 fM–178 pM	1.78 fM
CEA[152]	G-IDA/CPPy MNTs	FET	*	1 fg mL^{-1} – 1 ng mL^{-1}	1 fg mL^{-1}
17β-estradiol[153]	G-IDA/Ultrathin CPPy NTs	FET	*	1 fM – 1 nM	1 fM
As (III)[154]	G-IDA/CPPy coated flower-like MoS_2 nanospheres	FET	*	1 pM – 10 nM	1 pM
HBsAg[155]	Silver electrodes/Graphene/CPPy NW	FET	*	10 aM – 10 nM	10 aM
Dopamine[156]	IMEs/CPNTs	FET	*	----	100 pM
Adenosine Thrombin IFN-γ[173]	PPy NPs	Fluorescence	Ag nanocluster (i.e., labeled aptamer)	0 – 12.5 nM 2 – 25 nM 2 – 40 nM	0.39 nM 2.21 nM 0.58 nM
Kanamycin[177]	SPE/polyDPB-Au NPs nanocomposite	LSV	Kanamycin	0.05 µM - 9.0 µM	9.4 nM
17β-estradiol[175]	GCE/poly(Py-co-PAA)	EIS	$[Fe(CN)_6]^{3-/4-}$	----	1 fM
K^{+}[176]	GCE/poly(Py-co-PAA)	EIS	$[Fe(CN)_6]^{3-/4-}$	----	14.7 fM
Lysozyme[174]	GE/TiO_2/3D-rGO/PPy	DPV	$[Fe(CN)_6]^{3-/4-}$	0.1–50 ng mL^{-1} (0.007–3.5 nM).	0.085 ng mL^{-1} (5.5 pM)

Myoglobin[171]	GCE/PPy–Au nanocomposite	DPV	$[Fe(CN)_6]^{3-/4-}$	0.0001 - 0.15 g L^{-1}	30.9 ng mL^{-1}
S.Typhimurium[170]	GE/poly(Py-co-P3CA)	EIS	PPy (in $LiClO_4$ solution)	$10^2 – 10^8$ CFU mL^{-1}	3 CFU mL^{-1}
BPA[166]	poly(Py-NTA)-Cu^{2+}	SWV EIS	HQ	100 pM – 1 µM 10 pM - 1 µM	10 pM
OTA[167]	GE/CPPy/PAMAM	EIS	$[Fe(CN)_6]^{3-/4-}$	50 ng L^{-1} - 2 µg L^{-1}	2 ng L^{-1}
IL6[172]	SPE/PPy/Au NPs	EIS	$[Fe(CN)_6]^{3-/4-}$	1 pg mL^{-1} - 15 µg mL^{-1}	0.33 pg mL^{-1}
Cytochrome C[169]	SPE/Aptamer doped PPy	EIS	$[Fe(CN)_6]^{3-/4-}$	10 pM – 1 nM	5 pM
Pb (II)[165]	SPCE/Au@PPy	DPV	Toluidine Blue	0.5-25 ppb	0.6 ppb

VEGF: Vascular Endothelial Growth Factor. **IMEs**; interdigitated microelectrodes. **CPPy MNTs;** carboxylated polypyrrole multidimensional nanotubes . **DPB**: [2, 5-di-(2-thienyl)-1H-pyrrole-1-(p-benzoic acid)]. **PyNHP**: 3-N-hydroxyphthalimido pyrrole. **PDGF:** platelet-derived growth factor. **CPMCNF:** carboxylic polypyrrole-coated metal oxide-decorated carbon nanofibers. **cMb:** myoglobin protein antigen. **Py-co-PPa;** Pyrrole-co-pyrrolepropylic acid. **Py-co-P3CA;** Pyrrole and 3-carboxylated pyrrole monomers. **S.Typhimurium**: Salmonella Typhimurium. **BPA;** Bispheno A. **poly(Py-NTA);** poly(Pyrrole-Nitrilotriacetic Acid). **HQ;** Hydroquinone. **MNTs:** multidimentional nanotubes. **As;** Arsenic. **HBsAg:** Hepatitis B surface antigen. **NW:** nanowire. **SPCE**; Screen Printed Carbon Electrode. **ECL;** Electrochemiluminescence. **TPA;** Tripropylamine. **ErGO:** Electrochemically reduced Graphene Oxide. **PEC;** Photoelectrochemical. **AFB1:** Aflatoxin B1.
G-IDA; An interdigitated microelectrode array was patterned on a glass substrate. The IDA substrate was composed of a pair of gold interdigitated microelectrode. Then, the glass section is functionalized with PS /APTES and subsequently, with different nanostructures/modifier.
*I_{SD} source-drain current changes reflecting the binding event attributed to the modulation of charge carriers based on accumulation, or depletion modes,

iii. Polyindole (PIn) and PIn derivatives

The structural formula of "indole" was introduced by Baeyer and Emmerling in 1869.[178] Indole, as an aromatic heterocyclic compound, consists of a pyrrole ring fused to benzene to form 2,3-benzopyrrole that possesses the properties of both poly (para-phenylene) and PPy. In comparison to PANI and PPy, polyindole (PIn) has unique features including good thermal stability, long storage capability (especially in supercapacitor applications), and slow hydrolytic degradation.[179] Moreover, PIns offer excellent photoluminescent properties, highly stable redox activities, fast switching electrochromic properties, as well as air-stable electrical conductivity in the doped state.[180] However, the electrical and electrochemical conductivity of PIn is lower than that of PPy and PANI which restricts PIn-based devices

biosensing applications.[181] Among the many derivatives of PIn, poly (indole-carboxylic acid) (PICA) (Waltman et al., 1984)[182] and poly(5-formylindole) (P5FIn) (Nie et al., 2011)[183] are commonly used. The presence of electron-withdrawing carboxyl and aldehyde groups facilitates the monomer electrosynthesis and improves the polymer's stability on the electrode surface.[184] Moreover, the ease of covalent attachment of biorecognition elements, and intrinsic electrochemical activity at neutral pH (i.e., PICA) pave the way for developing biosensors in biological media.[185, 186] In recent years, Zhang et al. and Nie et al. have pioneered the detection of DNA hybridization by tracking PICA's intrinsic redox signal (in neutral media) using CV,[187] and investigating P5FIn-, PICA-based aptasensors using photoelectrochemical and electrochemiluminescence techniques.[160, 188-190] Combining the photoexcitation process with electrochemical detection renders PEC sensors with the unique advantage of being both optical and electrochemical sensors.[191] **Figure 8C** represents the photoelectrochemical detection of AFB1 (LOD = 0.002 ng mL^{-1}) using electrochemically reduced graphene oxide/poly(5-formylindole)/Au (erGO/P5FIn/Au) nanocomposite structure, with explaining the photocurrent generation mechanism.[160] A summary of some examples of PIn-based aptasensors is shown in Table 4.

Table 4. PIn-based Aptasensors

Analyte	PIn and its derivatives	Detection Method	Reporter Species/Signal Reporter	LDR	LOD
Ramos cells[188]	GCE/MWCNT/PICA	ECL	nanoprobe Au NPs/DNA/CdSe NPs	500 – 1.0 × 10^6 cells mL^{-1}	390 cells mL^{-1}

Ramos cells[189]	GCE/P5FIn	ECL	nanoprobe Au NPs/DNA/Ru(bpy)$_2$(dcbpy)NHS	500 – 1.0 × 10^5 cells mL^{-1}	300 cells mL^{-1}
AFB1[160]	ITO/Au Nanoflower/P5FIn/ErGO	PEC	Polymer composite	0.01 – 100 ng mL^{-1}	0.002 ng mL^{-1}
AFB1[190]	GCE/Au NRs/GQDs/PICA/F-Au NC	ECL	Polymer composite	0.01 – 100 ng mL^{-1}	3.75 pg mL^{-1}

Au NRs/GQDs/PICA/F-Au NC: Gold nanorods/graphene quantum dots-modified poly (indole-6-carboxylic acid)/flower-gold nanocomposite

iv. Polythiophene (PTh), PTh derivatives, and thiophene-based conjugated polyelectrolytes

As early as 1980, twenty years after the first attempt to synthesize polythiophenes (PThs), the electrical conductivity of the well-defined oxidized polythiophenes was simultaneously reported by Yamamoto, Lin, and Dudek.[192] From a theoretical point of view, PTh with a non-degenerate ground state, has been considered as a model for the study of charge transport in conducting polymers.[193] It is also of great interest in device applications due to its efficient electronic conjugation, high environmental stability of the (un)doped states, structural versatility, and solution processability.[194] The electronic band and chemical structures of polythiophene CPs, both p-type doping and n-type doping, were represented in **Figure. 9A**.[195]

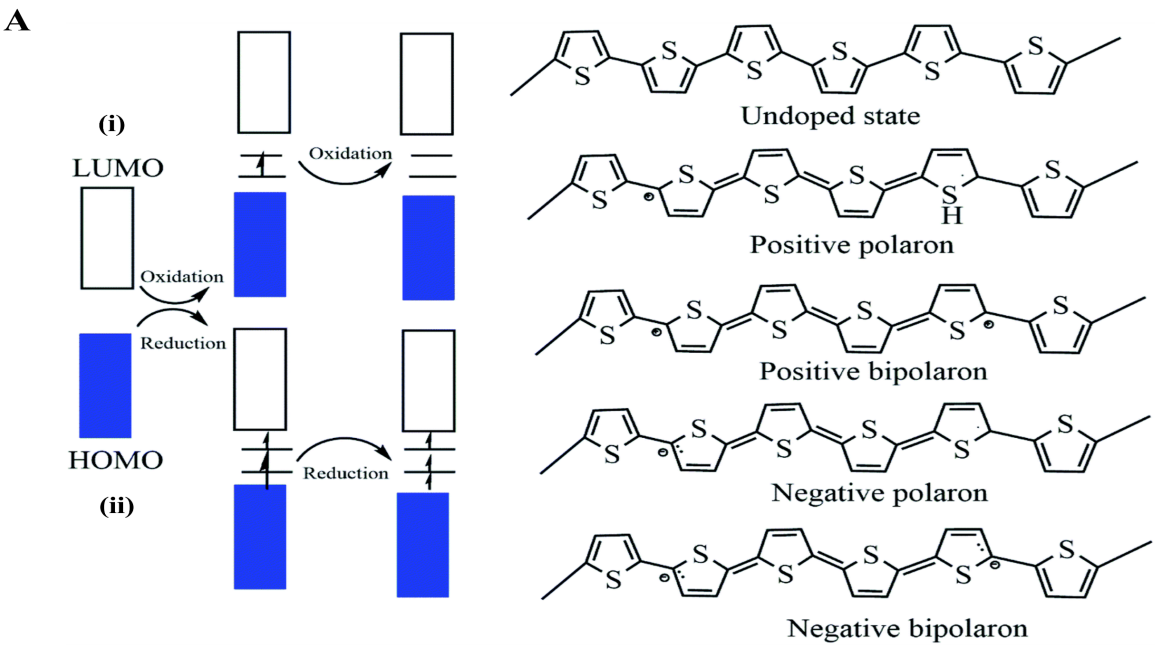
A
(i)
LUMO
Oxidation
Oxidation
Reduction
HOMO
Reduction
(ii)
Undoped state
Positive polaron
Positive bipolaron
Negative polaron
Negative bipolaron

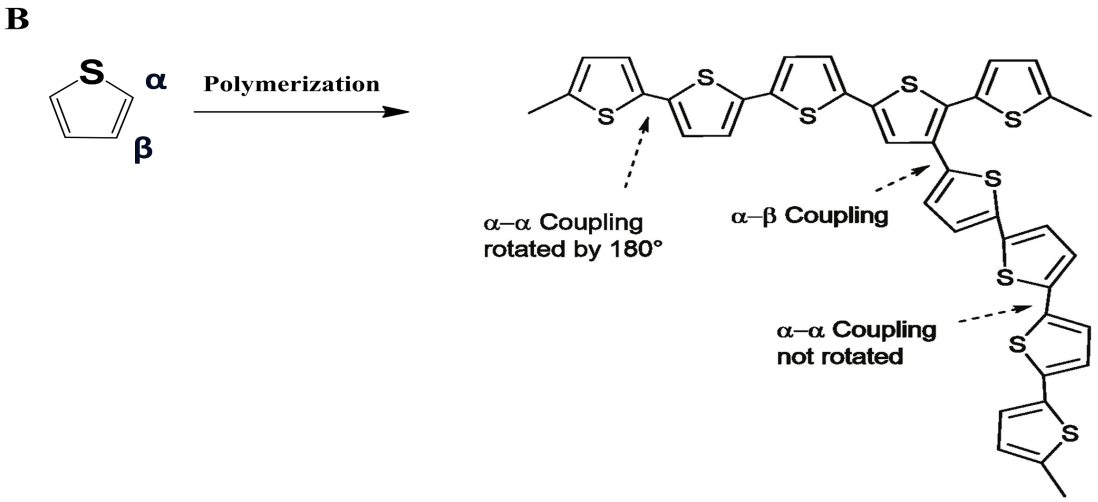
B
α
β
Polymerization
α–α Coupling
rotated by 180°
α–β Coupling
α–α Coupling
not rotated

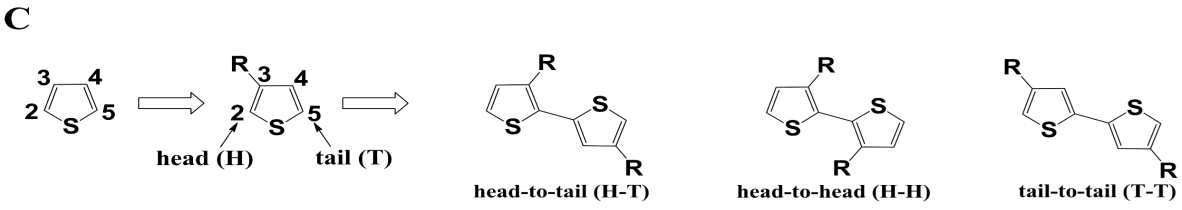
C
head (H)
tail (T)
head-to-tail (H-T)
head-to-head (H-H)
tail-to-tail (T-T)

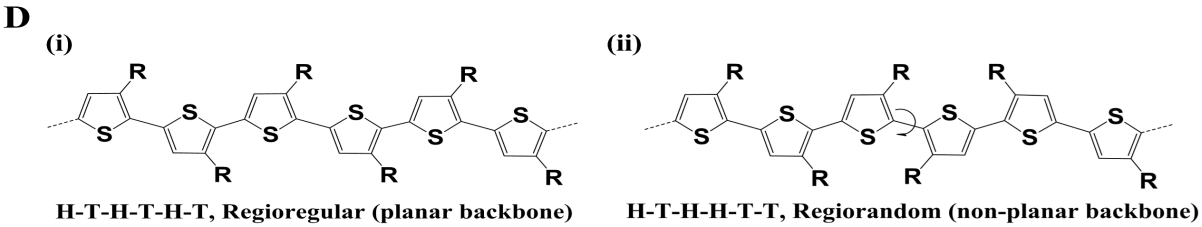
D
(i)
H-T-H-T-H-T, Regioregular (planar backbone)
(ii)
H-T-H-H-T-T, Regiorandom (non-planar backbone)

***Figure 9**. (A) Scheme of (i) p-type doping and (ii) n-type doping p-doping of polythiophene together with the evolution of its band gap. Adapted with permission under a Creative Commons (CC-BY 3.0) from Ref.[195] Copyright© 2021 Royal Chemical Society. (B) Possible polymerization form of thiophene during oxidation. Adapted with permission from Ref.[196] Copyright © 2019 Published by Elsevier Ltd. (C) Three possible coupling modes of 3-alkylthiophene units; Head-to-Tail (HT), Head-to-Head (HH), Tail-to-Tail (TT) (D) (i) Regioregular and (ii) Regiorandom orientation of polythiophene. Adapted with permission under a Creative Commons (CC-BY 4.0) from Ref.[197] Copyright© 2017 Nature.*

By the late 1980s, polymers of thiophenes containing different alkyl substituents were prepared,[198] which was followed by the introduction of the first water-soluble PThs derivatives,[199] and culminated by the synthesis of PEDOT.[200] The combination of convenient solution processability with high environmental stability, fast nonlinear optical (NLO) response, suitable crystallinity, good mechanical properties, and controllable conductivity is the main reasons for the introduction of substitutions in thiophene monomers that leads to the improvements of their electrical, optical, and physical properties.[201] Furthermore, the relatively high oxidation potential of the thiophene monomer leads to regiorandom coupling of its highly reactive cations during polymerization (**Figure 9B**), (i.e., results in the formation of highly insoluble polymers),[196] that could be avoided by the alkyl substitution of thiophene monomer (**Figure 9C**).[202, 203]

A study on 3-substituted thiophene has shown that its polymerization leads to the formation of a head-to-tail regioregularity with highly sterically favorable π-conjugation, which decreases the bandgap, improves micro-structural ordering and crystallinity in the solid-state and substantially enhances the electrical conductivity.[204] The use of thiophene monomers bearing substitutions offers several advantages; however, despite all their advantages, it is worth noting that the steric hindrance between 3- or/and 3,4-substituents could also form regioirregular polythiophenes that are twisted far out of conjugation

planarity that results in low electrical conductivity.[205] Different regiochemistry of 3-alkylthiophene units is displayed in **Figure 9D**. In this poly(heterocycle)'s structure, π-conjugation is perfectly extended in a 2,5'-linked repeating unit. However, a polymer backbone with a 2,2' and 5,5'-linked repeating unit can also be formed during polymerization that induces regiorandom conformation.[197] In contrast to 3-substituted polythiophenes for which routes to regioregular polymers are paved, analogous PPy is likely to have a mixture of regioisomers.[206]

Modifying the polymer backbone by incorporating diverse functional groups has proven to be a highly effective strategy for enhancing the sensory applications of polymers, especially in electrochemical methods. Shim's group pioneered the development of terthiophenes containing a functional group as a unit of the polymer backbone instead of thiophene.[207, 208] The first functionalized PThs-based electrochemical DNA sensor was developed by Shim et al. in 2001.[209] In this study, the newly synthesized PThs, 5,2′:5′2′′-terthiophene-3′-carboxylic acid (TTCA), was used for anchoring oligonucleotide probes via amide bond formation. This label-free detection strategy employed impedance measurements. Later, Shim and coworkers utilized poly-(2,2′:5′,5″-terthiophene-3′-p-benzoic acid (polyTTBA) decorated gold nanoparticles as an ultrasensitive cytosensor. The bioconjugate probe composed of MUC1 aptamer/Au NPs/hydrazine was employed to produce an electrocatalytic redox signal for the detection of MUC1 positive lung cancer cells (A549) in a sandwich architecture. An amperometric nano-biosensor enabled the achievement of a wide dynamic range from 15 to

1×10^6 cells mL^{-1} with a detection limit of 8 cells mL^{-1}.[210] Recently, polythiophene-bearing polyalanine homopeptide side chains (PTh-Pala) has also been successfully synthesized and applied for the electrochemical detection of cocaine.[211]

Talking about thiophene derivatives, PEDOT possesses intriguing features such as high conductivity and chemical stability in the oxidized state. It has been shown that the doped poly(cycloalkylenedioxythiophene)s are much more stable and have a bandgap lower than non- and alkyl-substituted polythiophene, owing to the presence of the two electron-donating oxygen atoms adjacent to the thiophene unit which not only decrease the bandgap by 0.5 eV but also increase the stabilization and rigidification via intramolecular non-covalent interactions between sulfur and oxygen atoms.[212, 213] Exploring the potential of PEDOT for aptasensing, Luo et al. reported the electrochemical detection of dopamine using a PEDOT-based aptasensor. In this approach, the graphene oxide-doped PEDOT (PEDOT-rGO) was electrochemically deposited on the electrode surface, followed by the electrochemical reduction of graphene oxide. Finally, detection of the target was accomplished by tracking the electrochemical signal of dopamine, which selectively binds to the immobilized aptamer on the PEDOT-rGO surface, and results in highly-sensitive detection of dopamine (LOD 78 fM) using DPV.[214] While PEDOT is insoluble in aqueous solutions, its polymerization with an anionic polyelectrolyte, such as poly(4-styrene sulfonate) (PSS), results in a stable aqueous PEDOT solution, with film-forming processability, high conductivity (ca. 10 S cm^{-1}), high light transmissivity, and good stability.

Further improvement of the conductivity of PEDOT:PSS is achieved by a post-treatment including thermal and light, acid, salt solution, ionic liquid, zwitterion treatment, and the addition of conducting nanoparticles and surfactants.[215] A broad range of aptasensors benefited from the PEDOT:PSS system characteristics. For example, Mayer et al. designed an interdigitated organic electrochemical transistor (iOECT), in which a PEDOT:PSS mixture formed the source-drain channel investigated in two modes.[216] In conventional mode, the electrochemical signal of the Fc-tagged aptamer, anchored on a gold surface, was traced in the presence of ATP. Upon binding to ATP, the Fc-tagged aptamer folded closer to the gold electrode surface, boosting the alternative cyclic voltammetry (ACV) signal, enabling LOD down to 106 nM. In another mode, the amperometric sensor was utilized as a gate electrode connected to the source-drain. Tracking the potential change of the gate electrode as a function of ATP concentration, a limit of detection of 10 pM was achieved (**Figure 10**).

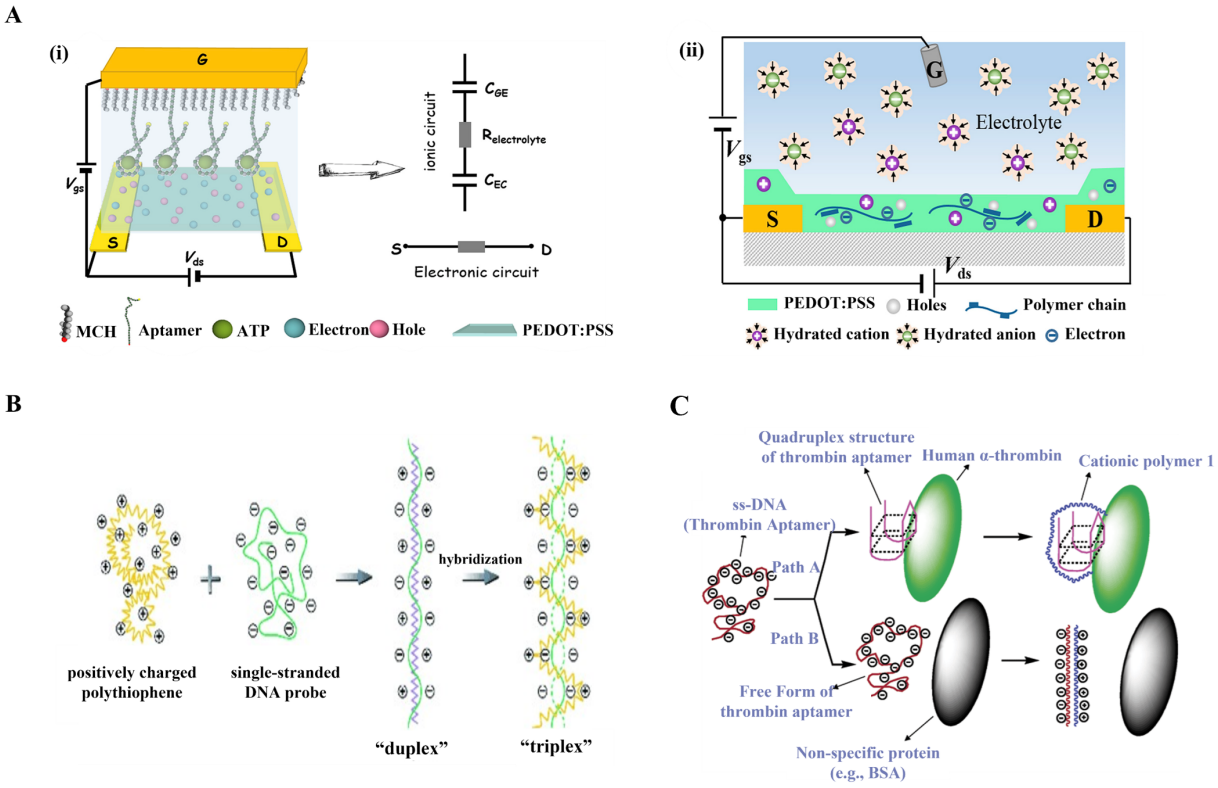

Figure 10. *(A) Schematic illustration of (i) an iOECT aptasensor for the detection of ATP with representation of two circuits for OECTs operation, ionic circuit and electronic circuit in which C_{GE} and C_{EC} related to the capacitances of two electrical double layers at the gate/electrolyte interface and electrolyte/channel interface, respectively. (ii) the cross-section of an iOECT transducer with PEDOT:PSS channel and Ag/AgCl wire as a gate electrode (G) representing the effect of a positive bias applied at the gate electrode. Adapted with permission from Ref.[216]. Copyright © 2019 Elsevier B.V. (B) Schematic description of (a) the formation of polythiophene/single-stranded nucleic acid duplex and polythiophene/hybridized nucleic acid triplex forms. Adapted with permission from Ref.[217] Copyright © 2002 WILEY-VCH Verlag GmbH, Weinheim, Fed. Rep. of Germany (C) the specific detection of human α-thrombin using ss-DNA thrombin aptamer and cationic polythiophene. Adapted with permission from Ref.[218]. Copyright © 2004, American Chemical Society.*

In addition to electrical conductivity, the excellent optoelectronic properties of PTh and its derivatives make them interesting in the colorimetric and fluorescent detection fields.[219] It has been reported that an electron-donating substitution on the thiophene ring leads to a polymer exhibiting a variety of colors in the neutral state or when oxidized.[220] Those types of CPs that combine optoelectronic and redox properties of conventional conjugated polymers with aqueous solubility and ionic nature of polyelectrolytes are called "conjugated polyelectrolytes" (CPEs) categorized in cationic conjugated polyelectrolytes (CCPEs) and

anionic conjugated polyelectrolytes (ACPEs)).[221] CPEs with poly(thiophene), poly(phenylene ethynylene) and poly(fluorene) backbones are the most common CPEs used for sensing purpose via fluorescence quenching, energy transfer, and based on conformational changes mechanism.[222-225] In 1987, Wudl synthesized the first CPEs by introducing the negative sulfonate groups into the terminal side chains of the polythiophene backbone.[199] Afterward, the report on application of water-soluble anionic CP, for the amplification of the sensitivity to fluorescence quenching was the pioneering study that laid the foundation for designing the CPE-based biological and chemical sensors.[226] Accordingly, Leclerc's group developed the first label-free colorimetric and fluorometric DNA sensor, aiming to link PTh derivatives to biological recognition elements in aqueous solutions.[217] They observed that the conformational change/aggregation of the newly synthesized cationic water-soluble poly(3-alkoxy-4-methylthiophenes), upon interaction with DNA, changes the solution color and the optical properties of PThs. In the former mode, the signal of pure polymer is red-shifted in the presence of target oligonucleotide and the obtained isosbestic point in the absorption spectra indicates the presence of only two distinct conformational structures (duplex and triplex) for the polymeric transducer. In parallel to colorimetric detection, the fluorometric assays showed that the fluorescence of cationic polymer is quenched in the planar, aggregated form (duplex) while upon hybridization, a polymeric triplex forms and leads to a fivefold rise in fluorescence intensity (**Figure 10B**). This simple procedure could provide fast and inexpensive methodologies for the rapid identification of perfectly matched and one-mismatched nucleic acids. In another report, they used the same cationic PThs to detect

specific targets that induce G-quadruplex conformation changes (e.g., aptamer/thrombin or aptamer/potassium ion). Based on different electrostatic interactions and conformational structures between CPE and single-stranded DNA (ssDNA), a simple and rapid strategy was proposed for the detection of thrombin (**Figure 10C**).[218] Currently, water-soluble PThs are becoming increasingly applicable in chemo- and biosensing since their chain conformations and photophysical properties are sensitive to external stimuli including thermal- or photo-treatment, the change of solvent composition, and the introduction of chemical and biochemical targets.[227] **Table 5** presents a brief overview of different PThs- and their derivatives-based biosensors.[211, 228-245]

Table 5. PTh-based Aptasensors

Analyte	PTh and its derivatives	Detection Method	Reporter Species/Signal Reporter	LDR	LOD
17β-Estradiol[236]	GE/PEDOT/Au NPs	SWV	$[Fe(CN)_6]^{3-/4-}$	0.1–100 nM	0.02 nM
Daunomycin[228]	GCE/Au NPs/PolyTTBA/PS-aptamer/AuNPs	DPV	Daunomycin	0.1 – 60 nM	52.3 pM
LPS[237]	GE/PolyEDTMSHA	EIS	$[Fe(CN)_6]^{3-/4-}$	0.1 – 1000 pg mL^{-1}	--
Pb^{2+}[235]	PMNT	Fluorescence	PMNT	10 – 120 nM	6 nM
Cocaine BE[211]	GCE/PT-Pala	DPV	$[Fe(CN)_6]^{3-/4-}$	2.5 - 10 nM 0.5 - 50 μM	 1.5 nM
Thrombin[240]	GE/3DOM C_{60}-PEDOT-IL	DPV	$[Fe(CN)_6]^{3-/4-}$	0.2 pM – 20 nM	0.02 pM
Thrombin[234]	PMNT	Colorimetry	TMB- H_2O_2	0.01–0.1 nM	4 pM
cTnI[231]	SPE/Au NPs/polyTTCA	Amperometry	H_2O_2	1–100 pM	1.0 pM

	Sandwich Assay (Hydrazine-labeled aptamer)			(0.024–2.4 ng mL^{-1})	(24 pg mL^{-1})
MPT64[239]	FTO/PEDOT-CNT	DPV	$[Fe(CN)_6]^{3-/4-}$	1.0×10^3 - 1.0×10^7 pg mL^{-1}	0.3 fg mL^{-1}
CCRF-CEM[238]	SPE/PEDOT-Au_{nano}	Amperometry	H_2O_2 Sandwich Assay (MWCNTs-Pdnano/PTCA/aptamer)	1.0×10^1 - 5.0×10^5 cells mL^{-1}	8 cells mL^{-1}
Thrombin[229]	SPE/polyTTBA	Amperometry	TBO Sandwich Assay (MNP@Ab-TBO)	1 - 500 nM	0.49 nM
OTA[244]	SPE/PT3C	EIS	$[Fe(CN)_6]^{3-/4-}$	0.125–2.5 ng ml^{-1}	0.125 ng mL^{-1}
MUC1[230]	FTO/Au-GO-PEDOT	DPV	$[Fe(CN)_6]^{3-/4-}$	3.13 aM – 31.25 nM (0.1 fg/mL – 1 µg/mL)	0.031 fM (1 fg mL^{-1})
NSE[242]	Carbon Electrode/PB-PEDOT-AuNPs	DPV	Prussian Blue	0.05 – 500 ng mL^{-1}	10 pg mL^{-1}
Malathion[232]	FTO/PEDOT-c-MWCNTs	DPV	$[Fe(CN)_6]^{3-/4-}$	0.1 fM – 1 mM	0.5 fM
ATP[233]	GCE/GO-PEDOT/Peptide (Antifouling)	DPV	$[Fe(CN)_6]^{3-/4-}$	0.1 pM - 1.0 µM	0.03 pM
OTA[241]	GOS/PEDOT-AuNFs	CV	$[Fe(CN)_6]^{3-/4-}$	0.01 - 20 ng L^{-1}	4.9 pg L^{-1}
AFB1[245]	PT3C	DPV	Methylene Blue (labeled aptamer)	2.5 - 30 ng L^{-1}	1.6 ng L^{-1}
CEA[243]	Paper/Graphene-PEDOT:PSS	EIS	$[Fe(CN)_6]^{3-/4-}$	0.77–14 ng mL^{-1}	0.45 ng mL^{-1}

ACV: Alternating Current Voltammetry (ACV), **Fc:** Ferrocene, **PS:** phosphatidylserine, **TTBA:** [2,2′:5,2″-terthiophene-3′-(p-benzoic acid)], **LPS:** Lipopolysaccharide, **EDTMSHA:** 3-((2,3-dihydrothieno[3,4b][1,4]dioxin-2-yl)methoxy)propane-1-thiol, **PMNT:** Poly [3-(30-N,N,N-triethylamino-10-propyloxy)-4-methyl-2,5-thiophene hydrochloride],**ErGO:** Electrochemically reduced Graphene Oxide, **BE:** Benzoylecgonine (Cocaine's metabolite), **Pala:** Polyalanine homopeptide, **T-Pala:** thiophene bearing polyalanine, , **cTnI:** Cardiac troponin I, **MPT64:** Mycobacterium tuberculosis (M. tb) antigen, **CCRM:** human leukemic lymphoblasts, **PTCA:** 3,4,9,10-perylene tetracarboxylic acid, **TBO:** Toluidine blue O,**c-MWCNTs:** carboxylated multi-walled carbon nanotubes, **OTA:** Ochratoxin A, GOS: Three-dimensional graphene oxide sponge, **PSS:** Poly(styrenesulfonate), **CEA:** Carcinoembryonic antigens, 3DOM: three-dimensional ordered microporous, **IL:** Ionic Liquids

v. Polyfluorene (PF) and PF derivatives and fluorene-based conjugated polyelectrolytes

The origin of polymer-based organic light-emitting diodes (OLED) was described by Burroughes et al. in 1990, based on poly(p-phenylenevinylene).[246] Since then, polyphenylene-based materials, particularly the blue-emitting category, became increasingly attractive ranging from unbridged (e.g., poly(para-phenylene) (PPP)) to the bridged polyphenylenes (i.e., from the simplest regular stepladder-type (e.g., polyfluorene; bridging between one bridge per two phenylenes) to fully bridged ladder-type polyphenylenes).[247, 248] Among them, polyfluorene (PF) and its derivatives have emerged as the most promising materials in the field of biosensing, more precisely in the optical field, with the potential to act not only as electroactive but also as photoactive polymers.[249] PFs, named "fluorene" owing to their supposed fluorescent property, contain a rigidly planar biphenyl structure enriched with abundant π-electrons in their backbone that leads to strong fluorescence emission.[250] High quantum efficiency, unique charge transport properties, excellent solubility, film-forming ability, good chemical, and thermal stability, and tunable properties through chemical modifications and copolymerization make PFs promising candidates in optoelectronic applications.[251] PFs can be tuned to emit throughout the entire visible spectrum via the incorporation of a chromophore in the main chain or substitutions of side chains in the 9,9-position of the fluorene unit. The acidity of the bridgehead (C9) protons in fluorene makes the alkylation process feasible at this position. Under phase transfer catalysis conditions, 9,9-dialkylfluorenes (DAFs) are obtained in high yield by treatment of fluorene with an alkyl halide and a base. To make PDAFs, both 4 and 5 can be used as monomers. (**Figure 11**).[248]

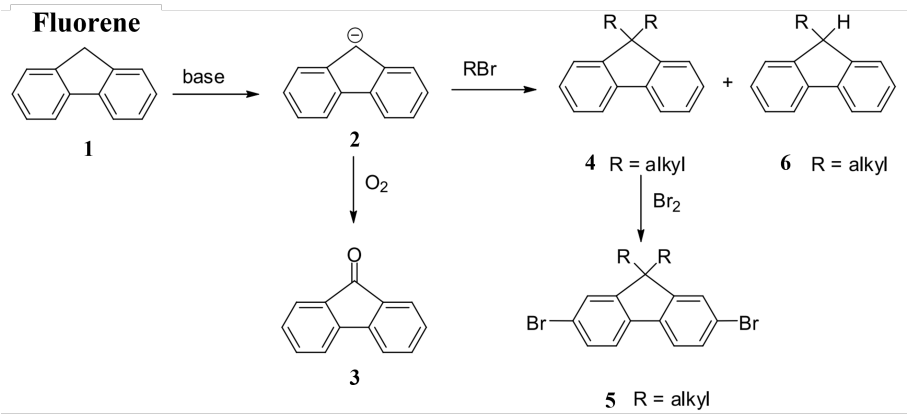

***Figure 11**. Alkylation of fluorine to produce monomers for PDAFs. (4 and 5 can be used as PDAFs' precursors). Adapted with permission from Ref.[248] Copyright © 2008, Springer-Verlag Berlin Heidelberg.*

Similar to other CPs, redox activity, charge transporting capabilities, optical absorption and emission, and chemical reactivity are some of the features provided by the introduction of side chains in PF structures. Additionally, the introduction of bulky side chains prevents agglomeration and induces solubility.[248, 252] Given the concept of conjugated polyelectrolyte structures, such side chains (e.g., pendant ionic functionalities) can also lead to the formation of CPEs.[253] The first water-soluble poly(p-phenylene) (PPP) derivative was reported by Novak. in 1991.[254] Phenylene-based polymers have since emerged as the focal point of biosensor research, employing optical methodologies. In line with this, Gaylord and coworkers reported the detection of DNA hybridization using water-soluble cationic CPE with poly(fluorene-co-phenylenene) backbone, poly(9,9-bis(6′-N,N,N-trimethylammonium)-hexyl)-fluorene phenylene) containing iodide counteranions in 2002.[255] The detection was performed based on fluorescence resonance energy transfer (FRET, reported in 1948 by a German physical chemist called Förster, which is a mechanism of energy transfer between two fluorophores (donor and acceptor) based on non-radiative

dipole-dipole interactions.[256] The hybridization of negatively charged DNA targets with fluorescein-labeled neutral peptide nucleic acid (PNA) brings CCPEs and duplex structures within distances suitable for FRET and results in an amplified optical signal. Nowadays, different types of cationic, anionic fluorene-based (co)polymers and polyfluorene dots (Pdots) have been developed and used for sensing applications through a variety of strategies. The chemical structures of fluorene-containing polymers mentioned in this section are depicted in **Figure 12**.

A

(i) PFVSO$_3$

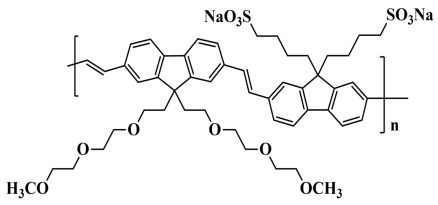

(ii) ThNI

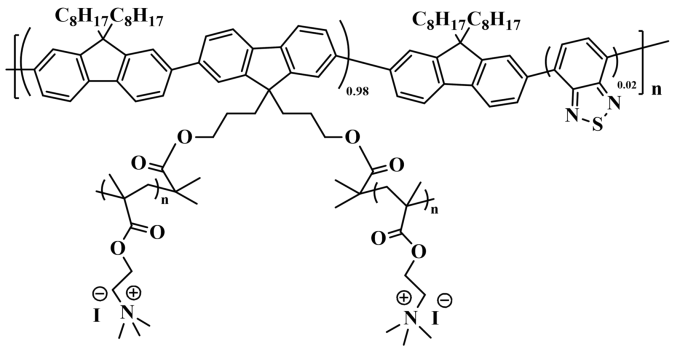

(iii) PFEP

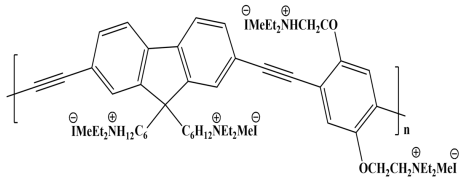

(iv) Cationic Tetrahedralfluorene

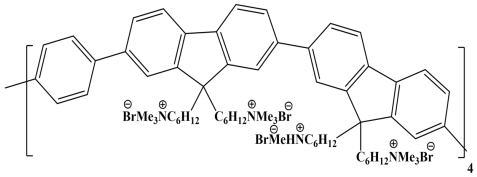

(v) PPFP-Br

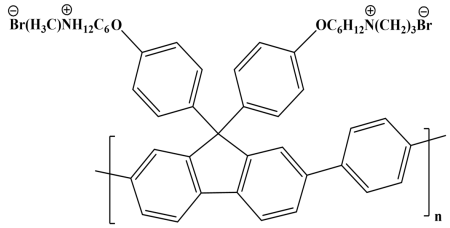

(vi) PFP

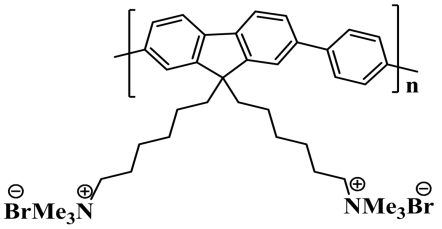

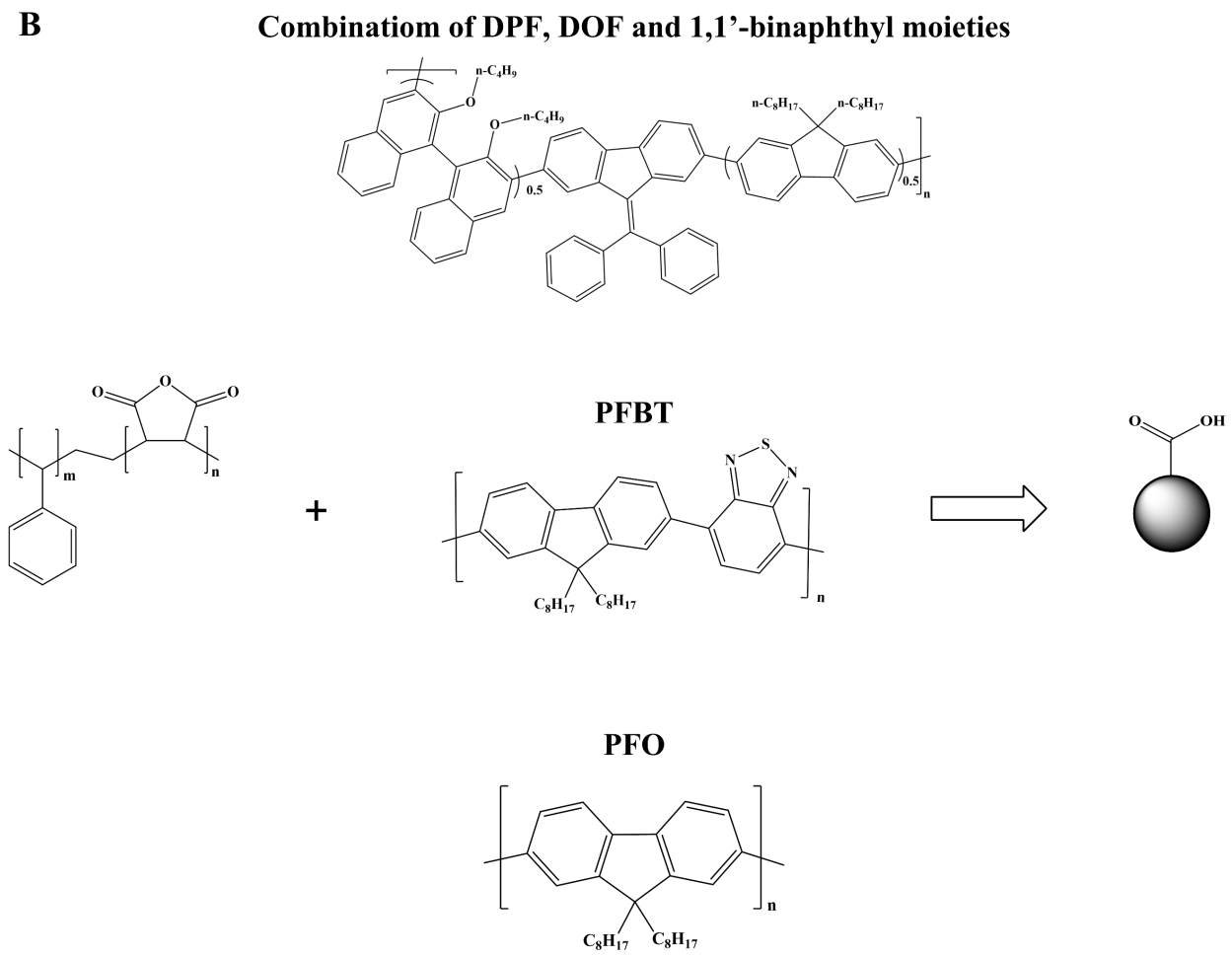

Figure 12. *Chemical structures of the variety of fluorene-based conjugated (A) polyelectrolytes (CPE) and, (B) polymer dots (Pdot) used for aptasensing approaches.*

Similarly, the application of fluorene-based CPEs has been explored for aptasensor development.[257] The first label-free detection of ATP was introduced by Wang et al. using cationic tetrahedralfluorene (tetrakis[4-(2-(9,9,9′,9′-tetrakis(N,N,N-trimethyl ammoniumhexyl)-7,2′-bifluorenyl))-phenyl]methane hexadecanebromide) as an energy donor as illustrated in **Figure 13A**.[258]

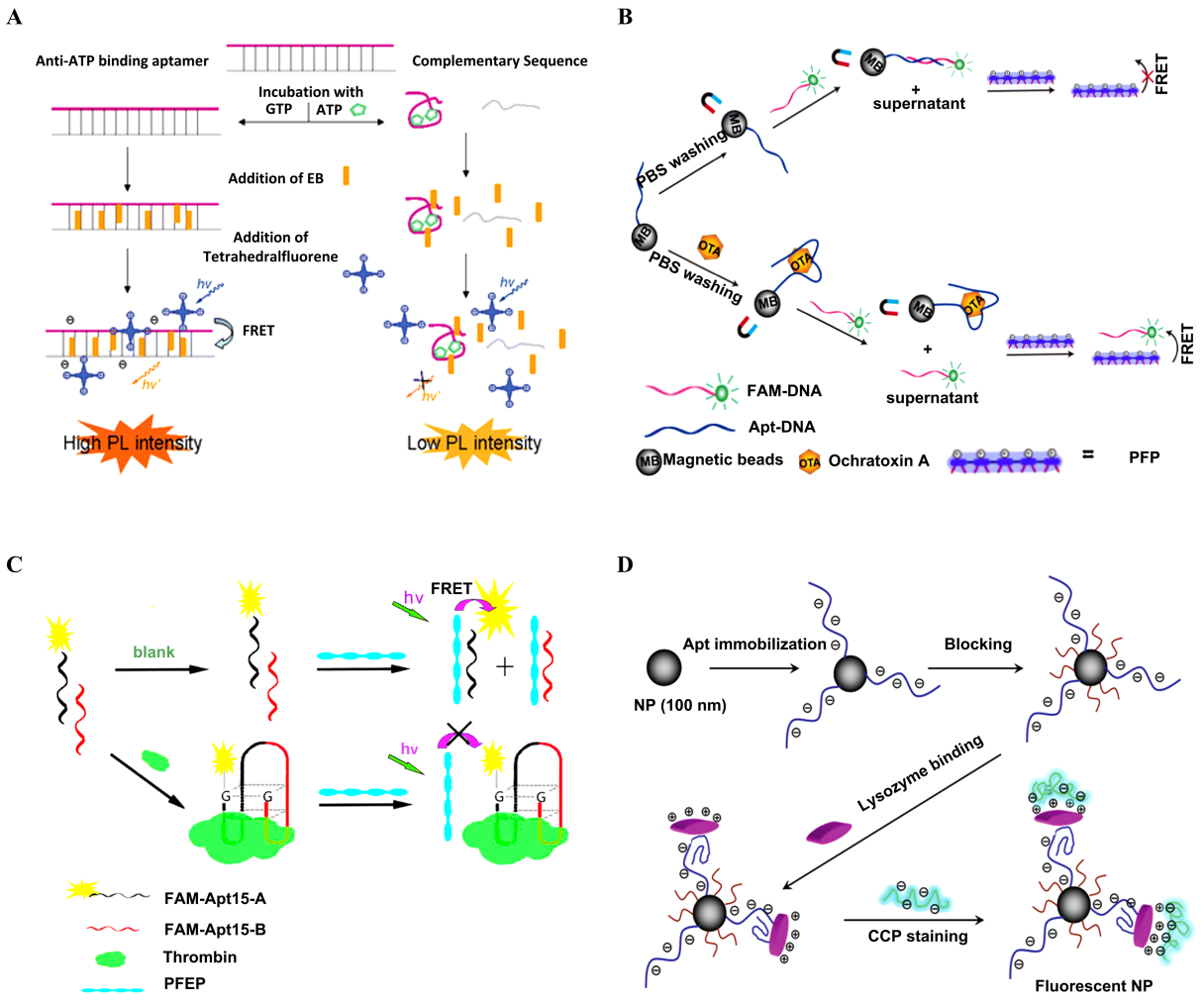

Figure. 13. *Schematic Illustration of (A) ATP detection using an aptamer and a cationic tetrahedralfluorene sensitized EB emission. Adapted with permission from Ref.[258]. Copyright © 2008, Royal Chemical Society. (B) fluorometric aptamer assay for the detection of OTA using CCPE and magnetic separation. Adapted with permission from Ref.[259]. Copyright © 2018, Springer-Verlag GmbH Austria, part of Springer Nature. (C) Thrombin detection based on the interaction of split aptamer fragments and PFEP. Adapted with permission from Ref.[260]. Copyright © 2014, American Chemical Society. (D) Label-free lysozyme detection with aptamer-immobilized silica NP and ACPE. Adapted with permission from Ref.[261]. Copyright © 2010, American Chemical Society.*

The study showed that the ATP-binding aptamer undergoes a conformational switch from "aptamer duplex" to "aptamer/target complex" upon binding to a target protein. In this study, the fluorescence emission of ethidium bromide (EB), that served as a signal reporter, is intensified when intercalated between aptamers. In the absence of a target, the addition of CCPEs sensitized the intercalated EB emission. As ATP opened the duplex-aptamer structure, CCPEs failed to efficiently enhance the emission of free EB in solution. This simple

methodology is employed for APT detection at LOD of 20 μM (**Figure 13A**). In biosensing experiments, matrix complexity is an undeniable issue that affects the technique's sensitivity. To overcome such challenges, Liu et al.[259] designed a FRET-based detection of OTA using magnetic beads (MBs) and CCPE **(Fig. 13B)**. In this method, the interaction of the target with the immobilized aptamer on MBs prevents the hybridization of short complementary FAM-labeled DNA and aptamers. The addition of PFP to the FAM-labeled DNA in the supernatant after magnetic separation leads to the efficient FRET from PFP to FAM, resulting in an amplified fluorescence signal and enhanced sensitivity for OTA detection.

Playing with the aptamer structure to develop a new sensing system, an aptasensor was designed based on the conformational change of an aptamer into the G-quadruplex structure upon target addition. Using two split aptamer fragments (one segment labeled with fluorescein (FAM)), Liu et al.[260] reported a signal-off biosensor for the detection of thrombin. In the absence of the target, the binding of FAM-labeled fragment aptamer to CPE led to a highly efficient FRET signal. However, in the presence of a target, two segments interact with the thrombin protein and combined to form a G-quadruplex structure. Due to the strong steric hindrance from the large-sized target protein, the distance between the water-soluble polycationic polymer (poly{[9,9-bis(6′-(N,N,N-diethylmethylammonium)hexyl)-2,7-fluorenylene ethynylene]-alt-co-[2,5-bis(3′-(N,N,N-diethylmethylammonium)-1′-oxapropyl)-1,4-phenylene] tetraiodide} (PFEP) and FAM increases, hence, the FRET signal decreases. The reported FRET biosensor reaches a LOD down to 2 nM for thrombin

detection (**Figure 13C**). Later, Wang et al. designed a sensing strategy for the detection of adenosine deaminase (ADA, at a low detection limit of 0.5 U/L) using the molecular aptamer beacon conformation and poly(9,9-bis(6′-N,N,N-trimethylammonium) hexyl)fluorine phenylene) (PFP).[262] Molecular beacon conformation is constituted of complementary nucleotide sequences in each stem which form hairpin-shaped structures. Aiming to be used in optical sensors, molecular beacons are labeled with a fluorescent dye in the 5′ end and a quencher molecule in the 3′ end. The hairpin-loop structure of the probes prevents fluorescence emission due to the proximity of the quencher and the fluorophore, which is resolved upon interaction with target analyte.[263, 264] Similarly, Kim et al. described a sensitive and selective detection of K^+ ions based on the conformational change of molecular beacon aptamer to either an open-chain form/a G-quadruplex in the absence/presence of K^+ ions.[265] Based on the recent observations, besides electrostatic interaction between negatively charged DNA and CCPEs, the hydrophobic interactions could also be driven since ssDNA is more flexible and significantly exposes more hydrophobic surface than double-stranded DNA (dsDNA).[266] Consistent with this, they introduced additional phenylene groups as a side chain into the PFP structure to improve the hydrophobic properties of the polymeric backbone to induce the conformational change of beacons from stem-loop to single-stranded structure in the absence of a target. Using this simple approach, the detection limit of 1.5 nM K^+ in the presence of 100 mM Na^+ was obtained.

In the application of anionic polyfluorene-based CPE, a novel aptamer-based sensing methodology was described to detect positively charged proteins by Wang et al. using ACPEs (**Figure 13D**).[261] They successfully developed highly fluorescent anionic poly(fluorene-alt-vinylene) ($PFVSO_3$) for lysozyme detection. Upon the interaction of lysozyme (pI~11.0, positively charged at neutral pH) with the immobilized aptamer on silica NPs (Apt-Si NPs), the surface charge of Apt-Si NPs switches from negative to partially positive. Consequently, the electrostatic interaction of anionic CPEs with Apt-NPs-lysozyme complexes leads to the emission of a blue-greenish fluorescence. The high quantum yield, the good water solubility of $PFVSO_3$, and effective isolation from interference are the main factors leading to the naked-eye lysozyme detection with picomole sensitivity (10 pmol).

Due to the major drawback of conventional fluorophores (e.g., organic dyes and QDs) including low absorptivity and poor photostability, low emission rates, blinking, difficulty in surface modification, and toxicity,[267-270] the fluorene-based CP dots have gained more attention in FRET-based aptasensing owing to their remarkable fluorescence brightness, unique light-harvesting, fast emission rate, and improved photostability, low toxicity and biocompatibility.[271-273] Taking these into account, Chiu et al. pioneered the use of CP dots in biological systems by controlling their surface chemistry via introducing functional groups on the CP dots' surface.[274] To achieve this goal, poly(styrene-co-maleic acid) (PSMA), as an amphiphilic functional part of the polymer, was introduced. Thereafter, Lin et al.[275] used poly(9,9-dioctylfluorenyl-2,7-diyl) dots (PFO dots) for the detection of carcinoembryonic

antigen (CEA) via FRET. In this method, the CEA aptamer links PFO dots and Au-NPs (acting as a quencher) through the immobilized ssDNA on their surface, which is partially complementary to the CEA aptamer, and formed a sandwich structure. Thereupon, the fluorescence intensity of PFO decreased, which is recovered after removing the quencher in the presence of CEA (0.1–10 ng mL^{-1}). **Table 6** provides a summary of other described PF-based aptasensor.[276-286]

Table 6. PF-based Aptasensors

Analyte	Fluorene-based CPs and CPEs	Detection Method/Mechanism	Signal Output Mode (On/Off)	LDR	LOD
Thrombin[282]	ThNI	Fluorescence FRET from the ThNI (donor) to ThT (G-quadruplex Inducer, fluorescent dye)	Off	0.02 - 2 nM	0.2 nM
ADA[284]	PFP	Fluorescence FRET from PFP (donor) to FAM (fluorescent dye) deoxyguanosines (Gs) (quencher, quenching FAM fluorescence via PET, in hairpin aptamer)	On	0.3 -150 U L^{-1}	0.3 U L^{-1}
AFB1[283]	PFBT-PSMA; Pdot	Fluorescence FRET from Pdots (donor) to Ag NPs (quencher)	On	5 – 1000 pg mL^{-1}	0.3 pg·mL^{-1}
Thrombin[286]	PFBT-PSMA; Pdot	Fluorescence FRET from Pdots (donor) to BHQ (quenching dye)	On	0-50 nM	0.33 nM
Pb (II)[276]	PSMA-DPF-DOF-BN; Pdot	ECL ECL emission of Pdots FRET from the excited DPF (donor) to RhB (quencher)	On	100 pM to 1.0 µM	38 pM
Streptavidin (SA)[285]	PFP	Fluorescence FRET from PFP (donor) to FAM (fluorescent dye) Graphene Oxide (quencher, quenching of FAM fluorescence)	On	2.0 – 100 ng mL−1	1.6 ng mL^{-1}
Lysozyme[279]	ThNI	Fluorescence FRET from ThNI (donor) to Au NPs (quencher)	On	1 nM – 25 nM	10 nM
Bisphenol A Dopamine[280]	PFP	Fluorescence FRET from PFP (donor) to FAM (fluorescent dye) Graphene Oxide (quencher, quenching of FAM fluorescence)	On	0 – 1.0 ng mL^{-1} 0 – 0.1 µM	0.005 ng mL^{-1} 1.0 nM
Thrombin[278]	PFP	Fluorescence	On	0.05 – 200 pM	0.05 pM

		FRET from CCP (donor) to Ir(III) complex (fluorescent complex)			
CEA Alpha Fetoprotein (AFP)[277]	PFN^+	Fluorescence	On	0.4 - 100 ng/mL --- 	0.316 ng mL^{-1} 1.76 ng mL^{-1}

ThNI; a polyfluorene derivative doped with benzothiazole**. ThT;** thioflavin T, a benzothiazole dye**. ADA**; adenosine deaminase (ADA). **Ag NPs:** silver nanoparticles. **Au NPs:** gold nanoparticles **BHQ**: black-hole quenching dye. **DFP-DOF-BN;** The polymer contained 9-(diphenylmethylene)-9H-fluorene (DPF), 9,9-dioctyl-9H-fluorene (DOF) and 1,1′-binaphthyl moieties. Ir(III) complex: (DFPPM-Ir-bpy-CO_2H)PF_6. **DFPPM**: 2-(2,4′-Difluorophenyl)pyrimidine **RhB:** rhodamine B **PFN^+;** Poly [(9, 9-bis (3′ -(dimethylethylaminonium) propyl)-2,7-fluorene dibromide].

3. CONCLUSION AND PERSPECTIVES.

Nowadays, conjugated polymers have a wide range of potential applications in various fields, including organic electronics, energy storage, photothermal therapy, antimicrobial coatings, tissue engineering, drug delivery, sensing, and biosensing due to their unique electronic, optical, and mechanical properties. Among them, their sensory application has gained remarkable attention in clinical diagnostics, food safety, and environmental monitoring. Despite all their advantages in sensing area, their selectivity remained a significant issue until the integration of aptamers as bio-recognition elements, which have proven to be a power horse for a myriad of biosensing applications. In addition, further improvement of the CP-based biosensor performance in terms of sensitivity and stability was achieved by the incorporation of nanomaterial, versatile dopants, or functionalization of corresponding monomers or polymers.

The purpose of this review was to explore conjugated polymers that are widely used in aptasensing and to gather different examples of the types of analytes detected in a variety of methodologies. Among all mentioned techniques, electrochemical and

fluorescence techniques are commonly used for the development of CP-based aptasensors. Ongoing efforts in this field are focused on enhancing the electrochemical activity and fluorescence properties of CPs. The development direction of conjugated polymers is focused on improving their performance and versatility for various applications. This involves developing new synthetic strategies for producing conjugated polymers with specific structures and properties, tuning their properties via modifying their chemical structure, optimizing their processing conditions for better film formation and device integration, and exploring new device architectures for achieving higher efficiency and functionality. Recently, significant progress has been made towards the development of donor-acceptor (D-A) conjugated polymers (i.e., featuring alternating donor and acceptor units along the polymer chain, resulting in a narrow bandgap and improved optoelectronic properties), the enhancement of biodegradability and biocompatibility of CPs (i.e., for sensory application, tissue engineering and drug delivery) and the production of highly stretchable CPs (e.g., flexible electronic devices). Accordingly, recent advancements have led to the demonstration of a new wearable CP-based aptasensor capable of real-time monitoring of essential biomolecules; PEDOT-based aptasensor designed for monitoring cortisol levels.

Overall, the application of conjugated polymers in biosensors is a rapidly evolving field with significant potential for a wide range of applications; in clinical trials, environmental assessment, and food analysis., opening up the path toward developing

sensitive and reliable analytical devices, which may eventually bridge the gap between on-site and real-time survey of environmental contaminations and point-of-care diagnosis of disease biomarkers. Ongoing research efforts are focused on developing new materials, improving sensor performance, and exploring new applications for these promising materials.

ASSOCIATED CONTENT

AUTHOR INFORMATION

Present Address:

#Department of Electronic & Electrical Engineering, University of Bath, Bath BA2 7AY, United Kingdom.

"For Table of Contents Use Only"

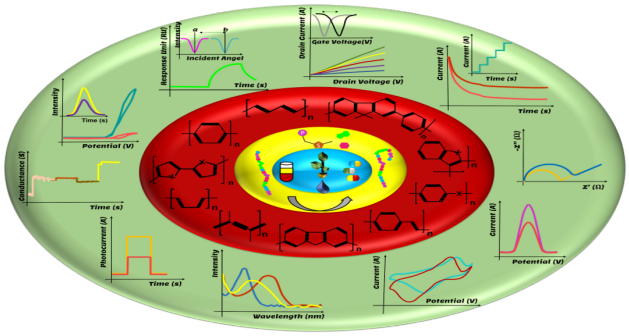

REFERENCES

1. Bhalla, N.; Jolly, P.; Formisano, N.; Estrela, P., Introduction to biosensors. *Essays Biochem* **2016,** 60, (1), 1-8.
2. Gowri, A.; Ashwin Kumar, N.; Suresh Anand, B. S., Recent advances in nanomaterials based biosensors for point of care (PoC) diagnosis of Covid-19 - A minireview. *Trends Analyt Chem* **2021,** 137, 116205.
3. Stephanie, R.; Kim, M. W.; Kim, S. H.; Kim, J.-K.; Park, C. Y.; Park, T. J., Recent advances of bimetallic nanomaterials and its nanocomposites for biosensing applications. *TrAC, Trends Anal. Chem.* **2021,** 135, 116159.
4. Lei, J.; Ju, H., Signal amplification using functional nanomaterials for biosensing. *Chem. Soc. Rev.* **2012,** 41, (6), 2122-2134.
5. Yang, L.; Zhang, S.; Liu, X.; Tang, Y.; Zhou, Y.; Wong, D. K. Y., Detection signal amplification strategies at nanomaterial-based photoelectrochemical biosensors. *J. Mater. Chem. B.* **2020,** 8, (35), 7880-7893.
6. Zhu, C.; Yang, G.; Li, H.; Du, D.; Lin, Y., Electrochemical Sensors and Biosensors Based on Nanomaterials and Nanostructures. *Anal. Chem.* **2015,** 87, (1), 230-249.
7. Xu, W.; Wang, D.; Li, D.; Liu, C. C., Recent Developments of Electrochemical and Optical Biosensors for Antibody Detection. *Int. J. Mol. Sci.* **2019,** 21, (1).
8. Naresh, V.; Lee, N., A review on biosensors and recent development of nanostructured materials-enabled biosensors. *Sensors* **2021,** 21, (4), 1109.
9. Arshad, M.; Zubair, M.; Rahman, S. S.; Ullah, A., Chapter 14 - Polymers for advanced applications. In *Polymer Science and Nanotechnology*, Narain, R., Ed. Elsevier: 2020; pp 325-340.
10. Balint, R.; Cassidy, N. J.; Cartmell, S. H., Conductive polymers: Towards a smart biomaterial for tissue engineering. *Acta Biomater.* **2014,** 10, (6), 2341-2353.
11. Maziz, A.; Özgür, E.; Bergaud, C.; Uzun, L., Progress in conducting polymers for biointerfacing and biorecognition applications. *Sens. Actuators Rep.* **2021,** 3, 100035.
12. Meng, L., *Tailoring Conducting Polymer Interface for Sensing and Biosensing*. Linköping University Electronic Press: 2020; Vol. 2094.
13. MacDiarmid, A. G.; Mammone, R.; Kaner, R.; Porter, L., The concept of 'doping'of conducting polymers: The role of reduction potentials. *Philos. Trans. R. Soc. London, Ser. A: Math. Phys. Sci.* **1985,** 314, (1528), 3-15.
14. Patil, A. O.; Heeger, A. J.; Wudl, F., Optical properties of conducting polymers. *Chem. Rev.* **1988,** 88, (1), 183-200.
15. Abu-Thabit, N. Y.; Makhlouf, A. S. H., Smart Textile Supercapacitors Coated with Conducting Polymers for Energy Storage Applications. In *Industrial Applications for Intelligent Polymers and Coatings*, Hosseini, M.; Makhlouf, A. S. H., Eds. Springer International Publishing: Cham, 2016; pp 437-477.
16. Bubnova, O.; Crispin, X., Towards polymer-based organic thermoelectric generators. *Energy Environ. Sci* **2012,** 5, (11), 9345-9362.
17. Walczak, R. M.; Cowart, J. S.; Reynolds, J. R., Tethered PProDOTs: conformationally restricted 3,4-propylenedioxythiophene based electroactive polymers. *J. Mater. Chem.* **2007,** 17, (3), 254-260.
18. Shahabuddin, M.; McDowell, T.; Bonner, C. E.; Noginova, N., Enhancement of Electrochromic Polymer Switching in Plasmonic Nanostructured Environment. *ACS Appl. Nano Mater.* **2019,** 2, (3), 1713-1719.
19. Mortimer, R. J., Electrochromic Materials. *Annu. Rev. Mater. Res.* **2011,** 41, (1), 241-268.
20. Sonmez, G., Polymeric electrochromics. *Chem. Commun.* **2005**, (42), 5251-5259.

21. John, S. V.; Iwuoha, E. I., Electrochromic Polymers for Solar Cells. In *Functional Polymers*, Jafar Mazumder, M. A.; Sheardown, H.; Al-Ahmed, A., Eds. Springer International Publishing: Cham, 2018; pp 1-36.
22. Ehsani, M.; Rahimi, P.; Joseph, Y., Structure–Function Relationships of Nanocarbon/Polymer Composites for Chemiresistive Sensing: A Review. *Sensors* **2021,** 21, (9), 3291.
23. Szeluga, U.; Kumanek, B.; Trzebicka, B., Synergy in hybrid polymer/nanocarbon composites. A review. *Compos. - A: Appl. Sci. Manuf.* **2015,** 73, 204-231.
24. Malhotra, B. D.; Ali, M. A., Nanomaterials in biosensors: Fundamentals and applications. *Nanomaterials for biosensors* **2018,** 1, 1-74.
25. Huang, X.; Zhu, Y.; Kianfar, E., Nano Biosensors: Properties, applications and electrochemical techniques. *J. Mater. Res. Technol.* **2021,** 12, 1649-1672.
26. BelBruno, J. J., Molecularly Imprinted Polymers. *Chem. Rev.* **2019,** 119, (1), 94-119.
27. Zhang, N.; Zhang, N.; Xu, Y.; Li, Z.; Yan, C.; Mei, K.; Ding, M.; Ding, S.; Guan, P.; Qian, L.; Du, C.; Hu, X., Molecularly Imprinted Materials for Selective Biological Recognition. *Macromol. Rapid Commun.* **2019,** 40, (17), e1900096.
28. Batista, A. D.; Silva, W. R.; Mizaikoff, B., Molecularly imprinted materials for biomedical sensing. *Med. Devices Sens.* **2021,** 4, (1), e10166.
29. Zhang, J.; Cao, Y., Chapter 6 - Aptasensors. In *Nano-Inspired Biosensors for Protein Assay with Clinical Applications*, Li, G., Ed. Elsevier: 2019; pp 139-166.
30. Chen, A.; Yang, S., Replacing antibodies with aptamers in lateral flow immunoassay. *Biosens. Bioelectron.* **2015,** 71, 230-242.
31. Crivianu-Gaita, V.; Thompson, M., Aptamers, antibody scFv, and antibody Fab' fragments: An overview and comparison of three of the most versatile biosensor biorecognition elements. *Biosens. Bioelectron.* **2016,** 85, 32-45.
32. Morales, M. A.; Halpern, J. M., Guide to Selecting a Biorecognition Element for Biosensors. *Bioconjugate Chem.* **2018,** 29, (10), 3231-3239.
33. Thiviyanathan, V.; Gorenstein, D. G., Aptamers and the next generation of diagnostic reagents. *Proteom. - Clin. Appl.* **2012,** 6, (11-12), 563-73.
34. Rimmele, M., Nucleic Acid Aptamers as Tools and Drugs: Recent Developments. *ChemBioChem* **2003,** 4, (10), 963-971.
35. Kaur, H.; Bruno, J. G.; Kumar, A.; Sharma, T. K., Aptamers in the Therapeutics and Diagnostics Pipelines. *Theranostics* **2018,** 8, (15), 4016-4032.
36. Bhardwaj, T.; Kumar Sharma, T., Aptasensors for full body health checkup. *Biosensors and Bioelectronics: X* **2022,** 11, 100199.
37. Xu, L.; Shoaie, N.; Jahanpeyma, F.; Zhao, J.; Azimzadeh, M.; Al Jamal, K. T., Optical, electrochemical and electrical (nano)biosensors for detection of exosomes: A comprehensive overview. *Biosens. Bioelectron.* **2020,** 161, 112222.
38. Song, S.-H.; Gao, Z.-F.; Guo, X.; Chen, G.-H., Aptamer-Based Detection Methodology Studies in Food Safety. *Food Anal. Methods* **2019,** 12, (4), 966-990.
39. Iqbal, S.; Ahmad, S., Recent development in hybrid conducting polymers: Synthesis, applications and future prospects. *J. Ind. Eng. Chem.* **2018,** 60, 53-84.
40. Marsitzky, D.; Müllen, K., 20 Years of "Synthetic Metals"–the Role of Synthesis. In *Advances in Synthetic Metals: Twenty Years of Progress in Science and Technology*, Bernier, P., Lefrant, S.,; Bidan, G., Eds. Elsevier: 1999; pp 1-98.
41. Shirakawa, H., Nobel Lecture: The discovery of polyacetylene film---the dawning of an era of conducting polymers. *Rev. Mod. Phys.* **2001,** 73, (3), 713-718.
42. Rasmussen, S., Low-Bandgap Polymers. In *Encyclopedia of Polymeric Nanomaterials*, Kobayashi, S.; Müllen, K., Eds. Springer Berlin Heidelberg: Berlin, Heidelberg, 2021; pp 1-13.

43. Hatano, M.; Kambara, S.; Okamoto, S., Paramagnetic and electric properties of polyacetylene. *J. Polym. Sci.* **1961,** 51, (156), S26-S29.
44. Spanggaard, H.; Krebs, F. C., A brief history of the development of organic and polymeric photovoltaics. *Sol. Energy Mater. Sol. Cells* **2004,** 83, (2), 125-146.
45. Chiang, C. K.; Park, Y. W.; Heeger, A. J.; Shirakawa, H.; Louis, E. J.; MacDiarmid, A. G., Conducting polymers: Halogen doped polyacetylene. *J. Chem. Phys.* **1978,** 69, (11), 5098-5104.
46. Shirakawa, H.; Louis, E. J.; MacDiarmid, A. G.; Chiang, C. K.; Heeger, A. J., Synthesis of electrically conducting organic polymers: halogen derivatives of polyacetylene, (CH). *J. Chem. Soc., Chem. Commun.* **1977**, (16), 578-580.
47. Heeger, A. J., Nobel Lecture: Semiconducting and metallic polymers: The fourth generation of polymeric materials. *Rev. Mod. Phys.* **2001,** 73, (3), 681.
48. Harlin, A.; Ferenets, M., Introduction to conductive materials. In *Intelligent textiles and clothing.*, Mattila H.R., Ed. Woodhed Puhlishing in Textiles: 2006; pp 217-238.
49. Boudrioua, A.; Chakaroun, M.; Fischer, A., *An introduction to organic lasers*. Elsevier: 2017.
50. Heydari Gharahcheshmeh, M.; Gleason, K. K., Texture and nanostructural engineering of conjugated conducting and semiconducting polymers. *Mater. Today Adv.* **2020,** 8, 100086.
51. Ahn, S.; Jeong, S.-H.; Han, T.-H.; Lee, T.-W., Conducting Polymers as Anode Buffer Materials in Organic and Perovskite Optoelectronics. *Adv. Opt. Mater.* **2017,** 5, (3), 1600512.
52. Wijeratne, K., *Conducting Polymer Electrodes for Thermogalvanic Cells*. Linköping University Electronic Press: 2019; Vol. 1971, p 7-30.
53. Megha, R.; Ali, F. A.; Ravikiran, Y. T.; Ramana, C. H. V. V.; Kiran Kumar, A. B. V.; Mishra, D. K.; Vijayakumari, S. C.; Kim, D., Conducting polymer nanocomposite based temperature sensors: A review. *Inorg. Chem. Commun.* **2018,** 98, 11-28.
54. Bredas, J. L.; Themans, B.; Andre, J. M.; Chance, R. R.; Silbey, R., The role of mobile organic radicals and ions (solitons, polarons and bipolarons) in the transport properties of doped conjugated polymers. *Synth. Met.* **1984,** 9, (2), 265-274.
55. Baleg, A. A.; Masikini, M.; John, S. V.; Williams, A. R.; Jahed, N.; Baker, P.; Iwuoha, E., Conducting Polymers and Composites. In *Functional Polymers*, Jafar Mazumder, M. A.; Sheardown, H.; Al-Ahmed, A., Eds. Springer International Publishing: Cham, 2018; pp 1-54.
56. Aldissi, M., Review of the synthesis of polyacetylene and its stabilization to ambient atmosphere. *Synth. Met.* **1984,** 9, (2), 131-141.
57. Friend, R. H., *Conductive Polymers II: From Science to Applications*. iSmithers Rapra Publishing: 1993; Vol. 2.
58. Mohammad, F., Chapter 8 - Stability of electrically conducting polymers. In *Handbook of Advanced Electronic and Photonic Materials and Devices*, Singh Nalwa, H., Ed. Academic Press: Burlington, 2001; pp 321-350.
59. Zeng, Q.; Jim, C. K. W.; Lam, J. W. Y.; Dong, Y.; Li, Z.; Qin, J.; Tang, B. Z., A new disubstituted polyacetylene for the detection of α-amino acids. *Macromol. Rapid Commun.* **2009,** 30, (3), 170-175.
60. Liu, Y.; Mills, R. C.; Boncella, J. M.; Schanze, K. S., Fluorescent polyacetylene thin film sensor for nitroaromatics. *Langmuir* **2001,** 17, (24), 7452-7455.
61. Sakai, R.; Satoh, T.; Kakuchi, T., Polyacetylenes as colorimetric and fluorescent chemosensor for anions. *Polym. Rev.* **2017,** 57, (1), 159-174.
62. Gui, M.; Jiang, J.; Wang, X.; Yan, Y.; Li, S.; Xiao, X.; Liu, T.; Liu, T.; Feng, Y., Copper ion-mediated glyphosate detection with N-heterocycle based polyacetylene as a sensing platform. *Sens. Actuators B: Chem* **2017,** 243, 696-703.
63. Lou, X.; Zeng, Q.; Zhang, Y.; Wan, Z.; Qin, J.; Li, Z., Functionalized polyacetylenes with strong luminescence:“turn-on” fluorescent detection of cyanide based on the dissolution of gold nanoparticles and its application in real samples. *J. Mater. Chem.* **2012,** 22, (12), 5581-5586.

64. Wegner, G.; Mitt, I., Polymerisation von Derivaten des 2.4-Hexadiin-1.6-diols im kristallinen Zustand. *Z. Naturforsch., Teil B* **1969,** 24, 824-832.
65. Jelinek, R.; Ritenberg, M., Polydiacetylenes–recent molecular advances and applications. *RSC Adv.* **2013,** 3, (44), 21192-21201.
66. Lee, J.; Jun, H.; Kim, J., Polydiacetylene–Liposome Microarrays for Selective and Sensitive Mercury(II) Detection. *Adv. Mater.* **2009,** 21, (36), 3674-3677.
67. Qian, X.; Städler, B., Recent Developments in Polydiacetylene-Based Sensors. *Chem. Mater.* **2019,** 31, (4), 1196-1222.
68. Wen, J. T.; Roper, J. M.; Tsutsui, H., Polydiacetylene Supramolecules: Synthesis, Characterization, and Emerging Applications. *Ind. Eng. Chem. Res.* **2018,** 57, (28), 9037-9053.
69. Sheth, S. R.; Leckband, D. E., Direct Force Measurements of Polymerization-Dependent Changes in the Properties of Diacetylene Films. *Langmuir* **1997,** 13, (21), 5652-5662.
70. Jelinek, R.; Kolusheva, S., Biomolecular Sensing with Colorimetric Vesicles. In *Creative Chemical Sensor Systems*, Schrader, T., Ed. Springer Berlin Heidelberg: Berlin, Heidelberg, 2007; pp 155-180.
71. Okada, S.; Peng, S.; Spevak, W.; Charych, D., Color and Chromism of Polydiacetylene Vesicles. *Acc. Chem. Res.* **1998,** 31, (5), 229-239.
72. Reichert, A.; Nagy, J. O.; Spevak, W.; Charych, D., Polydiacetylene Liposomes Functionalized with Sialic Acid Bind and Colorimetrically Detect Influenza Virus. *J. Am. Chem. Soc.* **1995,** 117, (2), 829-830.
73. Pan, J. J.; Charych, D., Molecular Recognition and Colorimetric Detection of Cholera Toxin by Poly(diacetylene) Liposomes Incorporating Gm1 Ganglioside. *Langmuir* **1997,** 13, (6), 1365-1367.
74. Bilby, D.; Kim, J., Self-Assembly of Conjugated Polymers and their Application to Biosensors. In *Supramolecular Soft Matter: Applications in Materials and Organic Electronics*, John Wiley & Sons, Inc. Hoboken, NJ, USA: 2011; pp 255-280.
75. Wen, J. T.; Bohorquez, K.; Tsutsui, H., Polydiacetylene-coated polyvinylidene fluoride strip aptasensor for colorimetric detection of zinc(II). *Sens. Actuators B: Chem.* **2016,** 232, 313-317.
76. Jung, Y. K.; Kim, T. W.; Park, H. G.; Soh, H. T., Specific Colorimetric Detection of Proteins Using Bidentate Aptamer-Conjugated Polydiacetylene (PDA) Liposomes. *Adv. Funct. Mater.* **2010,** 20, (18), 3092-3097.
77. Lee, J.; Kim, H.-J.; Kim, J., Polydiacetylene Liposome Arrays for Selective Potassium Detection. *J. Am. Chem. Soc.* **2008,** 130, (15), 5010-5011.
78. Wang, D.-E.; Gao, X.; You, S.; Chen, M.; Ren, L.; Sun, W.; Yang, H.; Xu, H., Aptamer-functionalized polydiacetylene liposomes act as a fluorescent sensor for sensitive detection of MUC1 and targeted imaging of cancer cells. *Sens. Actuators B: Chem.* **2020,** 309, 127778.
79. Wu, W.; Zhang, J.; Zheng, M.; Zhong, Y.; Yang, J.; Zhao, Y.; Wu, W.; Ye, W.; Wen, J.; Wang, Q., An aptamer-based biosensor for colorimetric detection of Escherichia coli O157: H7. *PloS one* **2012,** 7, (11), e48999.
80. Zhou, C.; You, T.; Jang, H.; Ryu, H.; Lee, E.-S.; Oh, M.-H.; Huh, Y. S.; Kim, S. M.; Jeon, T.-J., Aptamer-conjugated polydiacetylene colorimetric paper chip for the detection of Bacillus thuringiensis spores. *Sensors* **2020,** 20, (11), 3124.
81. Rasmussen, S. C., The early history of polyaniline: discovery and origins. *Substantia* **2017,** 1, (2), 99-109.
82. Huerta, F.; Quijada, C.; Montilla, F.; Morallón, E., Revisiting the Redox Transitions of Polyaniline. Semiquantitative Interpretation of Electrochemically Induced IR Bands. *J. Electroanal. Chem.* **2021,** 897, 115593.
83. Green, A. G.; Woodhead, A. E., CCXLIII.—Aniline-black and allied compounds. Part I. *J. Chem. Soc., Trans.* **1910,** 97, 2388-2403.

84. Inzelt, G., Historical Background (Or: There Is Nothing New Under the Sun). In *Conducting Polymers: A New Era in Electrochemistry*, Inzelt, G., Ed. Springer Berlin Heidelberg: Berlin, Heidelberg, 2012; pp 295-297.
85. De Surville, R.; Jozefowicz, M.; Yu, L. T.; Pepichon, J.; Buvet, R., Electrochemical chains using protolytic organic semiconductors. *Electrochim. Acta* **1968,** 13, (6), 1451-1458.
86. Diaz, A. F.; Logan, J. A., Electroactive polyaniline films. *J. electroanal. chem. interfacial electrochem.* **1980,** 111, (1), 111-114.
87. Bowmaker, G.; Gizdavic-Nikolaidis, M.; Zujovic, Z., *The Synthesis, Physical Properties, Bioactivity and Potential Applications of Polyanilines*. Cambridge Scholars Publishing: 2019.
88. Picciani, P. H. S.; Medeiros, E. S.; Orts, W. J.; Mattoso, L. H. C., *Advances in electroactive electrospun nanofibers*. InTech Rijeka: 2011; p 85-116.
89. Kurzweil, P., Secondary batteries. *Encyclopedia of electrochemical power sources. Elsevier, Amsterdam* **2009**, 565-578.
90. Le, T.-H.; Kim, Y.; Yoon, H., Electrical and electrochemical properties of conducting polymers. *Polymers* **2017,** 9, (4), 150.
91. Sapurina, I. Y.; Shishov, M. A., Oxidative Polymerization of Aniline: Molecular Synthesis of Polyaniline and the Formation of Supramolecular Structures. In *New Polymers for Special Applications*, Ailton De Souza, G., Ed. IntechOpen: Rijeka, 2012; p Ch. 9.
92. Gvozdenović, M. M.; Jugović, B.; Stevanović, J.; Grgur, B. N., Electrochemical synthesis of electroconducting polymers. *Hemijska industrija* **2014,** 68, (6), 673-684.
93. Tian, S.; Liu, J.; Zhu, T.; Knoll, W., Polyaniline/Gold Nanoparticle Multilayer Films: Assembly, Properties, and Biological Applications. *Chem. Mater.* **2004,** 16, (21), 4103-4108.
94. Luo, X.; Lee, I.; Huang, J.; Yun, M.; Cui, X. T., Ultrasensitive protein detection using an aptamer-functionalized single polyaniline nanowire. *Chem. Commun.* **2011,** 47, (22), 6368-6370.
95. Sen, T.; Mishra, S.; Shimpi, N. G., Synthesis and sensing applications of polyaniline nanocomposites: a review. *RSC Adv.* **2016,** 6, (48), 42196-42222.
96. Kazemi, F.; Naghib, S. M.; Mohammadpour, Z., Multifunctional micro-/nanoscaled structures based on polyaniline: an overview of modern emerging devices. *Mater. Today Chem.* **2020,** 16, 100249.
97. Liu, S.; Xing, X.; Yu, J.; Lian, W.; Li, J.; Cui, M.; Huang, J., A novel label-free electrochemical aptasensor based on graphene–polyaniline composite film for dopamine determination. *Biosens. Bioelectron.* **2012,** 36, (1), 186-191.
98. Karyakin, A. A.; Strakhova, A. K.; Yatsimirsky, A. K., Self-doped polyanilines electrochemically active in neutral and basic aqueous solutions.: Electropolymerization of substituted anilines. *J. Electroanal. Chem.* **1994,** 371, (1), 259-265.
99. Wang, Y.; Levon, K., Influence of Dopant on Electroactivity of Polyaniline. *Macromol. Symp.* **2012,** 317-318, (1), 240-247.
100. Tian, S.; Liu, J.; Zhu, T.; Knoll, W., Polyaniline doped with modified gold nanoparticles and its electrochemical properties in neutral aqueous solution. *Chem. Commun.* **2003**, (21), 2738-2739.
101. Liu, J.; Tian, S.; Knoll, W., Properties of Polyaniline/Carbon Nanotube Multilayer Films in Neutral Solution and Their Application for Stable Low-Potential Detection of Reduced β-Nicotinamide Adenine Dinucleotide. *Langmuir* **2005,** 21, (12), 5596-5599.
102. Zhou, H.; Lin, Y.; Yu, P.; Su, L.; Mao, L., Doping polyaniline with pristine carbon nanotubes into electroactive nanocomposite in neutral and alkaline media. *Electrochem. Commun.* **2009,** 11, (5), 965-968.
103. Su, Z.; Xu, X.; Xu, H.; Zhang, Y.; Li, C.; Ma, Y.; Song, D.; Xie, Q., Amperometric thrombin aptasensor using a glassy carbon electrode modified with polyaniline and multiwalled carbon nanotubes tethered with a thiolated aptamer. *Microchim. Acta* **2017,** 184, (6), 1677-1682.

104. Cajigas, S.; Orozco, J., Nanobioconjugates for signal amplification in electrochemical biosensing. *Molecules* **2020,** 25, (15), 3542.
105. Ravalli, A.; Voccia, D.; Palchetti, I.; Marrazza, G., Electrochemical, electrochemiluminescence, and photoelectrochemical aptamer-based nanostructured sensors for biomarker analysis. *Biosensors* **2016,** 6, (3), 39.
106. Bezinge, L.; Suea-Ngam, A.; deMello, A. J.; Shih, C.-J., Nanomaterials for molecular signal amplification in electrochemical nucleic acid biosensing: recent advances and future prospects for point-of-care diagnostics. *Mol. Syst. Des. Eng.* **2020,** 5, (1), 49-66.
107. Bai, L.; Chen, Y.; Bai, Y.; Chen, Y.; Zhou, J.; Huang, A., Fullerene-doped polyaniline as new redox nanoprobe and catalyst in electrochemical aptasensor for ultrasensitive detection of Mycobacterium tuberculosis MPT64 antigen in human serum. *Biomaterials* **2017,** 133, 11-19.
108. Wei, M.; Zhang, W., Ultrasensitive aptasensor with DNA tetrahedral nanostructure for Ochratoxin A detection based on hemin/G-quadruplex catalyzed polyaniline deposition. *Sens. Actuators B: Chem.* **2018,** 276, 1-7.
109. Zhang, Y.; Sun, X., A novel fluorescent aptasensor for thrombin detection: using poly(m-phenylenediamine) rods as an effective sensing platform. *Chem. Commun.* **2011,** 47, (13), 3927-3929.
110. Wen, Q.; Yang, P.-H., In situ electrochemical synthesis of Ni-capped electrochemiluminescence nanoprobe for ultrasensitive detection of cancer cells. *Anal. Methods.* **2015,** 7, (4), 1438-1445.
111. Stejskal, J., Polymers of phenylenediamines. *Prog. Polym. Sci.* **2015,** 41, 1-31.
112. Netsuwan, P.; Chaisu, W.; Phanichphant, S.; Sriwichai, S., Nanocomposite Thin Film of Poly(3-aminobenzoic acid) and Multiwalled Carbon Nanotubes Fabricated through an Electrochemical Method. *Adv. Mater. Sci. Eng.* **2014,** 2014, 873028.
113. Bai, L.; Yan, B.; Chai, Y.; Yuan, R.; Yuan, Y.; Xie, S.; Jiang, L.; He, Y., An electrochemical aptasensor for thrombin detection based on direct electrochemistry of glucose oxidase using a functionalized graphene hybrid for amplification. *Analyst* **2013,** 138, (21), 6595-6599.
114. Chen, X.; Zhang, Q.; Qian, C.; Hao, N.; Xu, L.; Yao, C., Electrochemical aptasensor for mucin 1 based on dual signal amplification of poly(o-phenylenediamine) carrier and functionalized carbon nanotubes tracing tag. *Biosens. Bioelectron.* **2015,** 64, 485-492.
115. Ensafi, A. A.; Khoddami, E.; Rezaei, B., Aptamer@Au-o-phenylenediamine modified pencil graphite electrode: A new selective electrochemical impedance biosensor for the determination of insulin. *Colloids Surf. B: Biointerfaces.* **2017,** 159, 47-53.
116. Fomo, G.; Waryo, T. T.; Sunday, C. E.; Baleg, A. A.; Baker, P. G.; Iwuoha, E. I., Aptameric recognition-modulated electroactivity of poly (4-styrenesolfonic acid)-doped polyaniline films for single-shot detection of tetrodotoxin. *Sensors* **2015,** 15, (9), 22547-22560.
117. Gao, H.; Xu, T.; Zhou, J.; Rojas, O. J.; He, M.; Ji, X.; Dai, H., Electrochemical sensing of Staphylococcus aureus based on conductive anti-fouling interface. *Microchim. Acta.* **2022,** 189, (3), 97.
118. Geleta, G. S.; Zhao, Z.; Wang, Z., A novel reduced graphene oxide/molybdenum disulfide/polyaniline nanocomposite-based electrochemical aptasensor for detection of aflatoxin B1. *Analyst* **2018,** 143, (7), 1644-1649.
119. Hashemi, P.; Bagheri, H.; Afkhami, A.; Ardakani, Y. H.; Madrakian, T., Fabrication of a novel aptasensor based on three-dimensional reduced graphene oxide/polyaniline/gold nanoparticle composite as a novel platform for high sensitive and specific cocaine detection. *Anal. Chim. Acta* **2017,** 996, 10-19.
120. Ji, X.; Yu, C.; Wen, Y.; Chen, J.; Yu, Y.; Zhang, C.; Gao, R.; Mu, X.; He, J., Fabrication of pioneering 3D sakura-shaped metal-organic coordination polymers Cu@L-Glu phenomenal for signal amplification in highly sensitive detection of zearalenone. *Biosens. Bioelectron.* **2019,** 129, 139-146.

121. Kulikova, T. N.; Porfireva, A. V.; Evtugyn, G. A.; Hianik, T., Electrochemical Aptasensor with Layer-by-layer Deposited Polyaniline for Aflatoxin M1 Voltammetric Determination. *Electroanalysis* **2019,** 31, (10), 1913-1924.
122. Lettieri, M.; Hosu, O.; Adumitrachioaie, A.; Cristea, C.; Marrazza, G., Beta-lactoglobulin electrochemical detection based with an innovative platform based on composite polymer. *Electroanalysis* **2020,** 32, (2), 217-225.
123. Li, Y.; Wang, L.; Ding, C.; Luo, X., Highly selective ratiometric electrogenerated chemiluminescence assay of DNA methyltransferase activity via polyaniline and anti-fouling peptide modified electrode. *Biosens. Bioelectron.* **2019,** 142, 111553.
124. Li, Z.; Yin, J.; Gao, C.; Qiu, G.; Meng, A.; Li, Q., The construction of electrochemical aptasensor based on coral-like poly-aniline and Au nano-particles for the sensitive detection of prostate specific antigen. *Sens. Actuators B: Chem.* **2019,** 295, 93-100.
125. Liu, N.; Song, J.; Lu, Y.; Davis, J. J.; Gao, F.; Luo, X., Electrochemical Aptasensor for Ultralow Fouling Cancer Cell Quantification in Complex Biological Media Based on Designed Branched Peptides. *Anal. Chem.* **2019,** 91, (13), 8334-8340.
126. Prabhakar, N.; Matharu, Z.; Malhotra, B. D., Polyaniline Langmuir–Blodgett film based aptasensor for ochratoxin A detection. *Biosens. Bioelectron.* **2011,** 26, (10), 4006-4011.
127. Rapini, R.; Cincinelli, A.; Marrazza, G., Acetamiprid multidetection by disposable electrochemical DNA aptasensor. *Talanta* **2016,** 161, 15-21.
128. Selvolini, G.; Lettieri, M.; Tassoni, L.; Gastaldello, S.; Grillo, M.; Maran, C.; Marrazza, G., Electrochemical enzyme-linked oligonucleotide array for aflatoxin B1 detection. *Talanta* **2019,** 203, 49-57.
129. Shahrokhian, S.; Ranjbar, S., Aptamer immobilization on amino-functionalized metal–organic frameworks: an ultrasensitive platform for the electrochemical diagnostic of Escherichia coli O157:H7. *Analyst* **2018,** 143, (13), 3191-3201.
130. Taleat, Z.; Cristea, C.; Marrazza, G.; Mazloum-Ardakani, M.; Săndulescu, R., Electrochemical immunoassay based on aptamer–protein interaction and functionalized polymer for cancer biomarker detection. *J. Electroanal. Chem.* **2014,** 717-718, 119-124.
131. Tertis, M.; Leva, P. I.; Bogdan, D.; Suciu, M.; Graur, F.; Cristea, C., Impedimetric aptasensor for the label-free and selective detection of Interleukin-6 for colorectal cancer screening. *Biosens. Bioelectron.* **2019,** 137, 123-132.
132. Wang, S.; Ma, Y.; Wang, Y.; Jiao, M.; Luo, X.; Cui, M., One-step electrodeposition of poly(m-aminobenzoic acid) membrane decorated with peptide for antifouling biosensing of Immunoglobulin E. *Colloids Surf. B: Biointerfaces.* **2020,** 186, 110706.
133. Wang, X.; Gao, F.; Gong, Y.; Liu, G.; Zhang, Y.; Ding, C., Electrochemical aptasensor based on conductive supramolecular polymer hydrogels for thrombin detection with high selectivity. *Talanta* **2019,** 205, 120140.
134. Wang, X.; Sun, D.; Tong, Y.; Zhong, Y.; Chen, Z., A voltammetric aptamer-based thrombin biosensor exploiting signal amplification via synergetic catalysis by DNAzyme and enzyme decorated AuPd nanoparticles on a poly(o-phenylenediamine) support. *Microchim. Acta.* **2017,** 184, (6), 1791-1799.
135. Wen, W.; Bao, T.; Yang, J.; Zhang, M.-Z.; Chen, W.; Xiong, H.-Y.; Zhang, X.-H.; Zhao, Y.-D.; Wang, S.-F., A novel amperometric adenosine triphosphate biosensor by immobilizing graphene/dual-labeled aptamers complex onto poly(o-phenylenediamine) modified electrode. *Sens. Actuators B: Chem.* **2014,** 191, 695-702.
136. Xiang, Y.; Zhang, Y.; Qian, X.; Chai, Y.; Wang, J.; Yuan, R., Ultrasensitive aptamer-based protein detection via a dual amplified biocatalytic strategy. *Biosens. Bioelectron.* **2010,** 25, (11), 2539-2542.

137. Xu, W.; Liu, S.; Yu, J.; Cui, M.; Li, J.; Guo, Y.; Wang, H.; Huang, J., An ultrasensitive HRP labeled competitive aptasensor for oxytetracycline detection based on grapheme oxide–polyaniline composites as the signal amplifiers. *RSC Adv.* **2014,** 4, (20), 10273-10279.
138. Xu, W.; Wang, Y.; Liu, S.; Yu, J.; Wang, H.; Huang, J., A novel sandwich-type electrochemical aptasensor for sensitive detection of kanamycin based on GR–PANI and PAMAM–Au nanocomposites. *New J. Chem.* **2014,** 38, (10), 4931-4937.
139. Ranjbar, S.; Nejad, M. A. F.; Parolo, C.; Shahrokhian, S.; Merkoçi, A., Smart Chip for Visual Detection of Bacteria Using the Electrochromic Properties of Polyaniline. *Anal. Chem.* **2019,** 91, (23), 14960-14966.
140. Rasmussen, S. C., Conjugated and Conducting Organic Polymers: The First 150 Years. *ChemPlusChem* **2020,** 85, (7), 1412-1429.
141. Rasmussen, S. C., Early history of conductive organic polymers. In *Conductive Polymers*, CRC Press: 2018; pp 1-22.
142. Iurchenkova, A. A.; Kallio, T.; Fedorovskaya, E. O., Relationships between polypyrrole synthesis conditions, its morphology and electronic structure with supercapacitor properties measured in electrolytes with different ions and pH values. *Electrochim. Acta* **2021,** 391, 138892.
143. Ansari, R., Polypyrrole Conducting Electroactive Polymers: Synthesis and Stability Studies. *J. Chem.* **2006,** 3, 860413.
144. Sasso, L.; Heiskanen, A.; Diazzi, F.; Dimaki, M.; Castillo-León, J.; Vergani, M.; Landini, E.; Raiteri, R.; Ferrari, G.; Carminati, M.; Sampietro, M.; Svendsen, W. E.; Emnéus, J., Doped overoxidized polypyrrole microelectrodes as sensors for the detection of dopamine released from cell populations. *Analyst* **2013,** 138, (13), 3651-3659.
145. Özkorucuklu, S. P.; Şahin, Y.; Alsancak, G., Voltammetric behaviour of sulfamethoxazole on electropolymerized-molecularly imprinted overoxidized polypyrrole. *Sensors* **2008,** 8, (12), 8463-8478.
146. Riande, E.; Díaz-Calleja, R., *Electrical properties of polymers*. CRC Press: 2004.
147. Korri-Youssoufi, H.; Garnier, F.; Srivastava, P.; Godillot, P.; Yassar, A., Toward Bioelectronics: Specific DNA Recognition Based on an Oligonucleotide-Functionalized Polypyrrole. *J. Am. Chem. Soc.* **1997,** 119, (31), 7388-7389.
148. Yoon, H.; Kim, J. H.; Lee, N.; Kim, B. G.; Jang, J., A novel sensor platform based on aptamer-conjugated polypyrrole nanotubes for label-free electrochemical protein detection. *Chembiochem* **2008,** 9, (4), 634-41.
149. Jun, J.; Lee, J. S.; Shin, D. H.; Jang, J., Aptamer-Functionalized Hybrid Carbon Nanofiber FET-Type Electrode for a Highly Sensitive and Selective Platelet-Derived Growth Factor Biosensor. *ACS Appl. Mater. Interfaces.* **2014,** 6, (16), 13859-13865.
150. Puri, N.; Niazi, A.; Biradar, A. M.; Mulchandani, A.; Rajesh, Conducting polymer functionalized single-walled carbon nanotube based chemiresistive biosensor for the detection of human cardiac myoglobin. *Appl. Phys. Lett.* **2014,** 105, (15), 153701.
151. Lee, J. S.; Kim, W.; Cho, S.; Jun, J.; Cho, K. H.; Jang, J., Multidimensional hybrid conductive nanoplate-based aptasensor for platelet-derived growth factor detection. *J. Mater. Chem. B.* **2016,** 4, (25), 4447-4454.
152. Park, J. W.; Na, W.; Jang, J., One-pot synthesis of multidimensional conducting polymer nanotubes for superior performance field-effect transistor-type carcinoembryonic antigen biosensors. *RSC Adv.* **2016,** 6, (17), 14335-14343.
153. Na, W.; Park, J. W.; An, J. H.; Jang, J., Size-controllable ultrathin carboxylated polypyrrole nanotube transducer for extremely sensitive 17β-estradiol FET-type biosensors. *J. Mater. Chem. B.* **2016,** 4, (29), 5025-5034.
154. An, J. H.; Jang, J., A highly sensitive FET-type aptasensor using flower-like MoS2 nanospheres for real-time detection of arsenic(iii). *Nanoscale* **2017,** 9, (22), 7483-7492.

155. Cho, K. H.; Shin, D. H.; Oh, J.; An, J. H.; Lee, J. S.; Jang, J., Multidimensional Conductive Nanofilm-Based Flexible Aptasensor for Ultrasensitive and Selective HBsAg Detection. *ACS Appl. Mater. Interfaces* **2018,** 10, (34), 28412-28419.
156. Park, S. J.; Lee, J.; Seo, S. E.; Kim, K. H.; Park, C. S.; Lee, S. H.; Ban, H. S.; Lee, B. D.; Song, H. S.; Kim, J.; Lee, C.-S.; Bae, J.; Kwon, O. S., High-Performance Conducting Polymer Nanotube-based Liquid-Ion Gated Field-Effect Transistor Aptasensor for Dopamine Exocytosis. *Sci. Rep.* **2020,** 10, (1), 3772.
157. Kwon, O. S.; Park, S. J.; Hong, J.-Y.; Han, A. R.; Lee, J. S.; Lee, J. S.; Oh, J. H.; Jang, J., Flexible FET-Type VEGF Aptasensor Based on Nitrogen-Doped Graphene Converted from Conducting Polymer. *ACS Nano* **2012,** 6, (2), 1486-1493.
158. Kwon, O. S.; Park, S. J.; Jang, J., A high-performance VEGF aptamer functionalized polypyrrole nanotube biosensor. *Biomaterials* **2010,** 31, (17), 4740-4747.
159. Miodek, A.; Castillo, G.; Hianik, T.; Korri-Youssoufi, H., Electrochemical aptasensor of cellular prion protein based on modified polypyrrole with redox dendrimers. *Biosens. Bioelectron.* **2014,** 56, 104-111.
160. Zhang, B.; Lu, Y.; Yang, C.; Guo, Q.; Nie, G., Simple "signal-on" photoelectrochemical aptasensor for ultrasensitive detecting AFB1 based on electrochemically reduced graphene oxide/poly(5-formylindole)/Au nanocomposites. *Biosens. Bioelectron.* **2019,** 134, 42-48.
161. Liao, W.; Randall, B. A.; Alba, N. A.; Cui, X. T., Conducting polymer-based impedimetric aptamer biosensor for in situ detection. *Anal. Bioanal. Chem.* **2008,** 392, (5), 861-864.
162. Ensafi, A. A.; Amini, M.; Rezaei, B., Molecularly imprinted electrochemical aptasensor for the attomolar detection of bisphenol A. *Microchim. Acta.* **2018,** 185, (5), 265.
163. Xu, H.; Gorgy, K.; Gondran, C.; Le Goff, A.; Spinelli, N.; Lopez, C.; Defrancq, E.; Cosnier, S., Label-free impedimetric thrombin sensor based on poly(pyrrole-nitrilotriacetic acid)-aptamer film. *Biosens. Bioelectron.* **2013,** 41, 90-95.
164. Hashemian, Z.; Khayamian, T.; Saraji, M.; Shirani, M. P., Aptasensor based on fluorescence resonance energy transfer for the analysis of adenosine in urine samples of lung cancer patients. *Biosens. Bioelectron.* **2016,** 79, 334-340.
165. Ding, J.; Zhang, D.; Liu, Y.; Yu, M.; Zhan, X.; Zhang, D.; Zhou, P., An electrochemical aptasensor for detection of lead ions using a screen-printed carbon electrode modified with Au/polypyrrole composites and toluidine blue. *Anal. Methods.* **2019,** 11, (33), 4274-4279.
166. Kazane, I.; Gorgy, K.; Gondran, C.; Spinelli, N.; Zazoua, A.; Defrancq, E.; Cosnier, S., Highly Sensitive Bisphenol-A Electrochemical Aptasensor Based on Poly(Pyrrole-Nitrilotriacetic Acid)-Aptamer Film. *Anal. Chem.* **2016,** 88, (14), 7268-7273.
167. Mejri-Omrani, N.; Miodek, A.; Zribi, B.; Marrakchi, M.; Hamdi, M.; Marty, J.-L.; Korri-Youssoufi, H., Direct detection of OTA by impedimetric aptasensor based on modified polypyrrole-dendrimers. *Anal. Chim. Acta* **2016,** 920, 37-46.
168. Miodek, A.; Poturnayová, A.; Šnejdárková, M.; Hianik, T.; Korri-Youssoufi, H., Binding kinetics of human cellular prion detection by DNA aptamers immobilized on a conducting polypyrrole. *Anal. Bioanal. Chem.* **2013,** 405, (8), 2505-2514.
169. Shafaat, A.; Faridbod, F.; Ganjali, M. R., Label-free detection of cytochrome C by a conducting polymer-based impedimetric screen-printed aptasensor. *New J. Chem.* **2018,** 42, (8), 6034-6039.
170. Sheikhzadeh, E.; Chamsaz, M.; Turner, A. P. F.; Jager, E. W. H.; Beni, V., Label-free impedimetric biosensor for Salmonella Typhimurium detection based on poly [pyrrole-co-3-carboxyl-pyrrole] copolymer supported aptamer. *Biosens. Bioelectron.* **2016,** 80, 194-200.
171. Sun, C.; Wang, D.; Geng, Z.; Gao, L.; Zhang, M.; Bian, H.; Liu, F.; Zhu, Y.; Wu, H.; Xu, W., One-step green synthesis of a polypyrrole–Au nanocomposite and its application in myoglobin aptasensor. *Anal. Methods.* **2015,** 7, (12), 5262-5268.

172. Tertiş, M.; Ciui, B.; Suciu, M.; Săndulescu, R.; Cristea, C., Label-free electrochemical aptasensor based on gold and polypyrrole nanoparticles for interleukin 6 detection. *Electrochim. Acta* **2017,** 258, 1208-1218.
173. Wang, J.; Li, B.; Lu, Q.; Li, X.; Weng, C.; Yan, X.; Hong, J.; Zhou, X., A versatile fluorometric aptasensing scheme based on the use of a hybrid material composed of polypyrrole nanoparticles and DNA-silver nanoclusters: application to the determination of adenosine, thrombin, or interferon-gamma. *Microchim. Acta.* **2019,** 186, (6), 356.
174. Wang, M.; Zhai, S.; Ye, Z.; He, L.; Peng, D.; Feng, X.; Yang, Y.; Fang, S.; Zhang, H.; Zhang, Z., An electrochemical aptasensor based on a TiO2/three-dimensional reduced graphene oxide/PPy nanocomposite for the sensitive detection of lysozyme. *Dalton Trans.* **2015,** 44, (14), 6473-6479.
175. Zhu, B.; Alsager, O. A.; Kumar, S.; Hodgkiss, J. M.; Travas-Sejdic, J., Label-free electrochemical aptasensor for femtomolar detection of 17β-estradiol. *Biosens. Bioelectron.* **2015,** 70, 398-403.
176. Zhu, B.; Booth, M. A.; Woo, H. Y.; Hodgkiss, J. M.; Travas-Sejdic, J., Label-Free, Electrochemical Quantitation of Potassium Ions from Femtomolar Levels. *Chem. Asian J.* **2015,** 10, (10), 2169-2175.
177. Zhu, Y.; Chandra, P.; Song, K.-M.; Ban, C.; Shim, Y.-B., Label-free detection of kanamycin based on the aptamer-functionalized conducting polymer/gold nanocomposite. *Biosens. Bioelectron.* **2012,** 36, (1), 29-34.
178. Van Order, R.; Lindwall, H., Indole. *Chem. Rev.* **1942,** 30, (1), 69-96.
179. Begum, B.; Bilal, S.; Shah, A. u. H. A.; Röse, P., Physical, chemical, and electrochemical properties of redox-responsive polybenzopyrrole as electrode material for faradaic energy storage. *Polymers* **2021,** 13, (17), 2883.
180. Thadathil, A.; Pradeep, H.; Joshy, D.; Ismail, Y. A.; Periyat, P., Polyindole and polypyrrole as a sustainable platform for environmental remediation and sensor applications. *Mater. Adv.* **2022,** 3, (7), 2990-3022.
181. Mudila, H.; Prasher, P.; Kumar, M.; Kumar, A.; Zaidi, M. G. H.; Kumar, A., Critical analysis of polyindole and its composites in supercapacitor application. *Mater. Renew. Sustain. Energy* **2019,** 8, (2), 9.
182. Waltman, R. J.; Diaz, A. F.; Bargon, J., Substituent effects in the electropolymerization of aromatic heterocyclic compounds. *J. Phys. Chem.* **1984,** 88, (19), 4343-4346.
183. Nie, G.; Zhou, L.; Yang, H., Electrosynthesis of a new polyindole derivative obtained from 5-formylindole and its electrochromic properties. *J. Mater. Chem.* **2011,** 21, (36), 13873-13880.
184. Ma, X.; Zhou, W.; Mo, D.; Lu, B.; Jiang, F.; Xu, J., One-step template-free electrodeposition of novel poly(indole-7-carboxylic acid) nanowires and their high capacitance properties. *RSC Adv.* **2015,** 5, (5), 3215-3223.
185. Nie, G.; Bai, Z.; Chen, J.; Yu, W., Simple Label-Free Femtomolar DNA Detection Based on a Nanostructure Composite Material: MWNT-Doped Poly(indole-6-carboxylic acid). *ACS Macro Lett.* **2012,** 1, (11), 1304-1307.
186. Zhang, W., Electrochemically reduced graphene oxide supported poly(indole-5-carboxylic acid) nanocomposite for genosensing application. *RSC Adv.* **2015,** 5, (125), 103649-103655.
187. Li, X.; Xia, J.; Zhang, S., Label-free detection of DNA hybridization based on poly(indole-5-carboxylic acid) conducting polymer. *Anal. Chim. Acta* **2008,** 622, (1), 104-110.
188. Nie, G.; Bai, Z.; Yu, W.; Zhang, L., Electrochemiluminescence biosensor for Ramos cells based on a nanostructured conducting polymer composite material (PICA-MWNTs). *J. Polym. Sci., Part A: Polym. Chem.* **2013,** 51, (11), 2385-2392.
189. Nie, G.; Bai, Z.; Yu, W.; Chen, J., Electrochemiluminescence Biosensor Based on Conducting Poly(5-formylindole) for Sensitive Detection of Ramos Cells. *Biomacromolecules* **2013,** 14, (3), 834-840.

190. Lu, Y.; Zhao, X.; Tian, Y.; Guo, Q.; Li, C.; Nie, G., An electrochemiluminescence aptasensor for the ultrasensitive detection of aflatoxin B1 based on gold nanorods/graphene quantum dots-modified poly(indole-6-carboxylic acid)/flower-gold nanocomposite. *Microchem. J.* **2020,** 157, 104959.
191. Ghosh, S.; Basu, R. N., Chapter 4 - Nanoscale Characterization. In *Noble Metal-Metal Oxide Hybrid Nanoparticles*, Mohapatra, S.; Nguyen, T. A.; Nguyen-Tri, P., Eds. Woodhead Publishing: 2019; pp 65-93.
192. Bidan, G., Electropolymerized Films of π-Conjugated Polymers. A Tool for Surface Functionalization: A Brief Historical Evolution and Recent Trends. In *Electropolymerization*, Wiley-VCH Verlag GmbH & Co. KGaA: 2010; pp 1-26.
193. Roncali, J., Conjugated poly (thiophenes): synthesis, functionalization, and applications. *Chem. Rev.* **1992,** 92, (4), 711-738.
194. Kaloni, T. P.; Giesbrecht, P. K.; Schreckenbach, G.; Freund, M. S., Polythiophene: From Fundamental Perspectives to Applications. *Chem. Mater.* **2017,** 29, (24), 10248-10283.
195. Namsheer, K.; Rout, C. S., Conducting polymers: A comprehensive review on recent advances in synthesis, properties and applications. *RSC Adv.,* **2021,** 11, (10), 5659-5697.
196. Thanasamy, D.; Jesuraj, D.; Konda kannan, S. K.; Avadhanam, V., A novel route to synthesis polythiophene with great yield and high electrical conductivity without post doping process. *Polymer* **2019,** 175, 32-40.
197. Ying, L.; Huang, F.; Bazan, G. C., Regioregular narrow-bandgap-conjugated polymers for plastic electronics. *Nat. Commun.* **2017,** 8, (1), 14047.
198. Elsenbaumer, R. L.; Jen, K. Y.; Oboodi, R., Processible and environmentally stable conducting polymers. *Synth. Met.* **1986,** 15, (2), 169-174.
199. Patil, A. O.; Ikenoue, Y.; Wudl, F.; Heeger, A. J., Water soluble conducting polymers. *J. Am. Chem. Soc.* **1987,** 109, (6), 1858-1859.
200. Bayer, A. G., Process for the preparation of polythiophenes. *European Patent* **1988,** 339340.
201. Mehmood, U.; Al-Ahmed, A.; Hussein, I. A., Review on recent advances in polythiophene based photovoltaic devices. *Renew. Sust. Energ. Rev.,* **2016,** 57, 550-561.
202. Jen, K.-Y.; Miller, G. G.; Elsenbaumer, R. L., Highly conducting, soluble, and environmentally-stable poly(3-alkylthiophenes). *J. Chem. Soc., Chem. Commun.* **1986**, (17), 1346-1347.
203. Amna, B.; Siddiqi, H. M.; Hassan, A.; Ozturk, T., Recent developments in the synthesis of regioregular thiophene-based conjugated polymers for electronic and optoelectronic applications using nickel and palladium-based catalytic systems. *RSC Adv.* **2020,** 10, (8), 4322-4396.
204. Facchetti, A.; Marks, T. J.; Katz, H. E.; Veinot, J., Organic Semiconductor Materials. In *Printed Organic and Molecular Electronics*, Gamota, D.; Brazis, P.; Kalyanasundaram, K.; Zhang, J., Eds. Springer US: Boston, MA, 2004; pp 83-159.
205. Tourillon, G.; Garnier, F., Structural effect on the electrochemical properties of polythiophene and derivatives. *J. electroanal. chem. interfacial electrochem.* **1984,** 161, (1), 51-58.
206. Wallace, G. G.; Teasdale, P. R.; Spinks, G. M.; Kane-Maguire, L. A. P., *Conductive electroactive polymers: intelligent materials systems*. CRC press: 2002.
207. Kim, D.-M.; Yoon, J.-H.; Won, M.-S.; Shim, Y.-B., Electrochemical characterization of newly synthesized polyterthiophene benzoate and its applications to an electrochromic device and a photovoltaic cell. *Electrochim. Acta* **2012,** 67, 201-207.
208. Lee, T.-Y.; Shim, Y.-B.; Shin, S. C., Simple preparation of terthiophene-3'-carboxylic acid and characterization of its polymer. *Synth. Met.* **2002,** 126, (1), 105-110.
209. Lee, T.-Y.; Shim, Y.-B., Direct DNA Hybridization Detection Based on the Oligonucleotide-Functionalized Conductive Polymer. *Anal. Chem.* **2001,** 73, (22), 5629-5632.

210. Mir, T. A.; Yoon, J.-H.; Gurudatt, N. G.; Won, M.-S.; Shim, Y.-B., Ultrasensitive cytosensing based on an aptamer modified nanobiosensor with a bioconjugate: Detection of human non-small-cell lung cancer cells. *Biosens. Bioelectron.* **2015,** 74, 594-600.
211. Bozokalfa, G.; Akbulut, H.; Demir, B.; Guler, E.; Gumus, Z. P.; Odaci Demirkol, D.; Aldemir, E.; Yamada, S.; Endo, T.; Coskunol, H.; Timur, S.; Yagci, Y., Polypeptide Functional Surface for the Aptamer Immobilization: Electrochemical Cocaine Biosensing. *Anal. Chem.* **2016,** 88, (7), 4161-4167.
212. Pei, Q.; Zuccarello, G.; Ahlskog, M.; Inganäs, O., Electrochromic and highly stable poly(3,4-ethylenedioxythiophene) switches between opaque blue-black and transparent sky blue. *Polymer* **1994,** 35, (7), 1347-1351.
213. Roncali, J.; Blanchard, P.; Frère, P., 3,4-Ethylenedioxythiophene (EDOT) as a versatile building block for advanced functional π-conjugated systems. *J. Mater. Chem.* **2005,** 15, (16), 1589-1610.
214. Wang, W.; Wang, W.; Davis, J. J.; Luo, X., Ultrasensitive and selective voltammetric aptasensor for dopamine based on a conducting polymer nanocomposite doped with graphene oxide. *Microchim. Acta.* **2015,** 182, (5), 1123-1129.
215. Alcácer, L., Case study: PEDOT:PSS. In *Electronic Structure of Organic Semiconductors*, Morgan & Claypool Publishers: 2018; pp 9-1-9-15.
216. Liang, Y.; Wu, C.; Figueroa-Miranda, G.; Offenhäusser, A.; Mayer, D., Amplification of aptamer sensor signals by four orders of magnitude via interdigitated organic electrochemical transistors. *Biosens. Bioelectron.* **2019,** 144, 111668.
217. Ho, H. A.; Boissinot, M.; Bergeron, M. G.; Corbeil, G.; Doré, K.; Boudreau, D.; Leclerc, M., Colorimetric and fluorometric detection of nucleic acids using cationic polythiophene derivatives. *Angew. Chem.* **2002,** 114, (9), 1618-1621.
218. Ho, H.-A.; Leclerc, M., Optical Sensors Based on Hybrid Aptamer/Conjugated Polymer Complexes. *J. Am. Chem. Soc.* **2004,** 126, (5), 1384-1387.
219. Das, S.; Chatterjee, D. P.; Ghosh, R.; Nandi, A. K., Water soluble polythiophenes: preparation and applications. *RSC Adv.* **2015,** 5, (26), 20160-20177.
220. Skotheim, T. A.; Reynolds, J., *Conjugated polymers: theory, synthesis, properties, and characterization*. CRC press: 2006.
221. Mikroyannidis, J. A.; Barberis, V. P.; Cimrová, V., Novel electroluminescent cationic polyelectrolyte based on poly[(fluorene-2,7-diylvinylene)-alt-(1,4-phenylenevinylene)] and its precursor. *J. Polym. Sci., Part A: Polym. Chem.* **2007,** 45, (6), 1016-1027.
222. Lemieux, É. J.; Leclerc, M., Sensing via Conformational Changes of Conjugated Polythiophenes. In *Conjugated Polyelectrolytes*, Wiley-VCH Verlag GmbH & Co. KGaA: 2012; pp 231-261.
223. Lv, F.; Wang, S.; Bazan, G. C., Sensing Applications via Energy Transfer from Conjugated Polyelectrolytes. In *Conjugated Polyelectrolytes*, Wiley-VCH Verlag GmbH & Co. KGaA: 2012; pp 201-229.
224. Wu, D.; Yang, J.; Feng, F.; Schanze, K. S., Sensing via Quenching of Conjugated Polyelectrolyte Fluorescence. In *Conjugated Polyelectrolytes*, Wiley-VCH Verlag GmbH & Co. KGaA: 2012; pp 169-200.
225. Zalar, P.; Nguyen, T.-Q., Charge Injection Mechanism in PLEDs and Charge Transport in Conjugated Polyelectrolytes. In *Conjugated Polyelectrolytes*, Wiley-VCH Verlag GmbH & Co. KGaA: 2012; pp 315-344.
226. Chen, L.; McBranch, D. W.; Wang, H.-L.; Helgeson, R.; Wudl, F.; Whitten, D. G., Highly sensitive biological and chemical sensors based on reversible fluorescence quenching in a conjugated polymer. *Proc. Natl. Acad. Sci.* **1999,** 96, (22), 12287-12292.
227. Li, C.; Shi, G., Polythiophene-Based Optical Sensors for Small Molecules. *ACS Appl. Mater. Interfaces* **2013,** 5, (11), 4503-4510.
228. Chandra, P.; Noh, H.-B.; Won, M.-S.; Shim, Y.-B., Detection of daunomycin using phosphatidylserine and aptamer co-immobilized on Au nanoparticles deposited conducting polymer. *Biosens. Bioelectron.* **2011,** 26, (11), 4442-4449.

229. Chung, S.; Moon, J.-M.; Choi, J.; Hwang, H.; Shim, Y.-B., Magnetic force assisted electrochemical sensor for the detection of thrombin with aptamer-antibody sandwich formation. *Biosens. Bioelectron.* **2018,** 117, 480-486.
230. Gupta, P.; Bharti, A.; Kaur, N.; Singh, S.; Prabhakar, N., An electrochemical aptasensor based on gold nanoparticles and graphene oxide doped poly(3,4-ethylenedioxythiophene) nanocomposite for detection of MUC1. *J. Electroanal. Chem.* **2018,** 813, 102-108.
231. Jo, H.; Her, J.; Lee, H.; Shim, Y.-B.; Ban, C., Highly sensitive amperometric detection of cardiac troponin I using sandwich aptamers and screen-printed carbon electrodes. *Talanta* **2017,** 165, 442-448.
232. Kaur, N.; Thakur, H.; Prabhakar, N., Multi walled carbon nanotubes embedded conducting polymer based electrochemical aptasensor for estimation of malathion. *Microchem. J.* **2019,** 147, 393-402.
233. Li, Z.; Yin, J.; Gao, C.; Sheng, L.; Meng, A., A glassy carbon electrode modified with graphene oxide, poly(3,4-ethylenedioxythiophene), an antifouling peptide and an aptamer for ultrasensitive detection of adenosine triphosphate. *Microchim. Acta* **2019,** 186, (2), 90.
234. Liu, M.; Li, J.; Li, B., A colorimetric aptamer biosensor based on cationic polythiophene derivative as peroxidase mimetics for the ultrasensitive detection of thrombin. *Talanta* **2017,** 175, 224-228.
235. Lu, Y.; Li, X.; Wang, G.; Tang, W., A highly sensitive and selective optical sensor for Pb2+ by using conjugated polymers and label-free oligonucleotides. *Biosens. Bioelectron.* **2013,** 39, (1), 231-235.
236. Olowu, R. A.; Arotiba, O.; Mailu, S. N.; Waryo, T. T.; Baker, P.; Iwuoha, E., Electrochemical aptasensor for endocrine disrupting 17β-estradiol based on a poly (3, 4-ethylenedioxylthiopene)-gold nanocomposite platform. *Sensors* **2010,** 10, (11), 9872-9890.
237. Su, W.; Cho, M.; Nam, J.-D.; Choe, W.-S.; Lee, Y., Aptamer-Assisted Gold Nanoparticles/PEDOT Platform for Ultrasensitive Detection of LPS. *Electroanalysis* **2013,** 25, (2), 380-386.
238. Amouzadeh Tabrizi, M.; Shamsipur, M.; Saber, R.; Sarkar, S., Flow injection amperometric sandwich-type aptasensor for the determination of human leukemic lymphoblast cancer cells using MWCNTs-Pdnano/PTCA/aptamer as labeled aptamer for the signal amplification. *Anal. Chim. Acta* **2017,** 985, 61-68.
239. Thakur, H.; Kaur, N.; Sareen, D.; Prabhakar, N., Electrochemical determination of M. tuberculosis antigen based on Poly(3,4-ethylenedioxythiophene) and functionalized carbon nanotubes hybrid platform. *Talanta* **2017,** 171, 115-123.
240. Tian, R.; Chen, X.; Li, Q.; Yao, C., An electrochemical aptasensor electrocatalyst for detection of thrombin. *Anal. Biochem.* **2016,** 500, 73-79.
241. Wang, P.; Wang, L.; Ding, M.; Pei, M.; Guo, W., Ultrasensitive electrochemical detection of ochratoxin A based on signal amplification by one-pot synthesized flower-like PEDOT–AuNFs supported on a graphene oxide sponge. *Analyst* **2019,** 144, (19), 5866-5874.
242. Wang, Y.; Luo, J.; Liu, J.; Sun, S.; Xiong, Y.; Ma, Y.; Yan, S.; Yang, Y.; Yin, H.; Cai, X., Label-free microfluidic paper-based electrochemical aptasensor for ultrasensitive and simultaneous multiplexed detection of cancer biomarkers. *Biosens. Bioelectron.* **2019,** 136, 84-90.
243. Yen, Y.-K.; Chao, C.-H.; Yeh, Y.-S., A graphene-PEDOT: PSS modified paper-based aptasensor for electrochemical impedance spectroscopy detection of tumor marker. *Sensors* **2020,** 20, (5), 1372.
244. Zejli, H.; Goud, K. Y.; Marty, J. L., Label free aptasensor for ochratoxin A detection using polythiophene-3-carboxylic acid. *Talanta* **2018,** 185, 513-519.
245. Zejli, H.; Goud, K. Y.; Marty, J. L., An electrochemical aptasensor based on polythiophene-3-carboxylic acid assisted methylene blue for aflatoxin B1 detection. *Sens. Bio-Sens. Res.* **2019,** 25, 100290.
246. Burroughes, J. H.; Bradley, D. D. C.; Brown, A. R.; Marks, R. N.; Mackay, K.; Friend, R. H.; Burns, P. L.; Holmes, A. B., Light-emitting diodes based on conjugated polymers. *Nature* **1990,** 347, (6293), 539-541.

247. Grimsdale, A. C.; Müllen, K., Polyphenylene-type Emissive Materials: Poly(para-phenylene)s,Polyfluorenes, and Ladder Polymers. In *Emissive Materials Nanomaterials*, Springer Berlin Heidelberg: Berlin, Heidelberg, 2006; pp 1-82.
248. Grimsdale, A. C.; Müllen, K., Bridged Polyphenylenes – from Polyfluorenes to Ladder Polymers. In *Polyfluorenes*, Scherf, U.; Neher, D., Eds. Springer Berlin Heidelberg: Berlin, Heidelberg, 2008; pp 1-48.
249. Leclerc, M., Polyfluorenes: Twenty years of progress. *J. Polym. Sci., Part A: Polym. Chem.* **2001,** 39, (17), 2867-2873.
250. Neher, D., Polyfluorene Homopolymers: Conjugated Liquid-Crystalline Polymers for Bright Blue Emission and Polarized Electroluminescence. *Macromol. Rapid Commun.* **2001,** 22, (17), 1365-1385.
251. Kappaun, S.; Slugovc, C.; List, E. J. W., Optically Active Chemical Defects in Polyfluorene-Type Polymers and Devices. In *Polyfluorenes*, Scherf, U.; Neher, D., Eds. Springer Berlin Heidelberg: Berlin, Heidelberg, 2008; pp 273-292.
252. Reynolds, J. R., Pi-conjugated polymers: The importance of polymer synthesis. In *Conjugated Polymers: A Practical Guide to Synthesis*, RSC Publishing: 2013; Vol. 1, pp 1-11.
253. Bazan, G. C.; Henson, Z., Conjugated Polyelectrolytes. In *Encyclopedia of Polymeric Nanomaterials*, Kobayashi, S.; Müllen, K., Eds. Springer Berlin Heidelberg: Berlin, Heidelberg, 2015; pp 427-433.
254. Wallow, T. I.; Novak, B. M., In aqua synthesis of water-soluble poly (p-phenylene) derivatives. *J. Am. Chem. Soc.* **1991,** 113, (19), 7411-7412.
255. Gaylord, B. S.; Heeger, A. J.; Bazan, G. C., DNA detection using water-soluble conjugated polymers and peptide nucleic acid probes. *Proc. Natl. Acad. Sci.* **2002,** 99, (17), 10954-10957.
256. Sapsford, K. E.; Berti, L.; Medintz, I. L., Materials for Fluorescence Resonance Energy Transfer Analysis: Beyond Traditional Donor–Acceptor Combinations. *Angew. Chem. Int. Ed.* **2006,** 45, (28), 4562-4589.
257. Liu, B.; Bazan, G. C., Homogeneous Fluorescence-Based DNA Detection with Water-Soluble Conjugated Polymers. *Chem. Mater.* **2004,** 16, (23), 4467-4476.
258. Wang, Y.; Liu, B., ATP detection using a label-free DNA aptamer and a cationic tetrahedralfluorene. *Analyst* **2008,** 133, (11), 1593-1598.
259. Liu, Y.; Yan, H.; Shangguan, J.; Yang, X.; Wang, M.; Liu, W., A fluorometric aptamer-based assay for ochratoxin A using magnetic separation and a cationic conjugated fluorescent polymer. *Microchim. Acta* **2018,** 185, (9), 427.
260. Liu, X.; Shi, L.; Hua, X.; Huang, Y.; Su, S.; Fan, Q.; Wang, L.; Huang, W., Target-Induced Conjunction of Split Aptamer Fragments and Assembly with a Water-Soluble Conjugated Polymer for Improved Protein Detection. *ACS Appl. Mater. Interfaces* **2014,** 6, (5), 3406-3412.
261. Wang, Y.; Pu, K.-Y.; Liu, B., Anionic Conjugated Polymer with Aptamer-Functionalized Silica Nanoparticle for Label-Free Naked-Eye Detection of Lysozyme in Protein Mixtures. *Langmuir* **2010,** 26, (12), 10025-10030.
262. Wang, C.; Tang, Y.; Liu, Y.; Guo, Y., Water-Soluble Conjugated Polymer as a Platform for Adenosine Deaminase Sensing Based on Fluorescence Resonance Energy Transfer Technique. *Anal. Chem.* **2014,** 86, (13), 6433-6438.
263. Tyagi, S.; Kramer, F. R., Molecular Beacons: Probes that Fluoresce upon Hybridization. *Nat. Biotechnol.* **1996,** 14, (3), 303-308.
264. Lomonaco, S., IDENTIFICATION METHODS | Application of Single Nucleotide Polymorphisms–Based Typing for DNA Fingerprinting of Foodborne Bacteria. In *Encyclopedia of Food Microbiology (Second Edition)*, Batt, C. A.; Tortorello, M. L., Eds. Academic Press: Oxford, 2014; pp 289-294.
265. Kim, B.; Jung, I. H.; Kang, M.; Shim, H.-K.; Woo, H. Y., Cationic Conjugated Polyelectrolytes-Triggered Conformational Change of Molecular Beacon Aptamer for Highly Sensitive and Selective Potassium Ion Detection. *J. Am. Chem. Soc.* **2012,** 134, (6), 3133-3138.

266. Xia, F.; Zuo, X.; Yang, R.; Xiao, Y.; Kang, D.; Vallée-Bélisle, A.; Gong, X.; Heeger, A. J.; Plaxco, K. W., On the Binding of Cationic, Water-Soluble Conjugated Polymers to DNA: Electrostatic and Hydrophobic Interactions. *J. Am. Chem. Soc.* **2010,** 132, (4), 1252-1254.
267. Hardman, R., A Toxicologic Review of Quantum Dots: Toxicity Depends on Physicochemical and Environmental Factors. *Environ. Health Perspect.* **2006,** 114, (2), 165-172.
268. Jin, S.; Hu, Y.; Gu, Z.; Liu, L.; Wu, H.-C., Application of quantum dots in biological imaging. *J. Nanomaterials* **2011,** 2011, 1-13.
269. Resch-Genger, U.; Grabolle, M.; Cavaliere-Jaricot, S.; Nitschke, R.; Nann, T., Quantum dots versus organic dyes as fluorescent labels. *Nat. Methods* **2008,** 5, (9), 763-775.
270. Wu, C.; Schneider, T.; Zeigler, M.; Yu, J.; Schiro, P. G.; Burnham, D. R.; McNeill, J. D.; Chiu, D. T., Bioconjugation of Ultrabright Semiconducting Polymer Dots for Specific Cellular Targeting. *J. Am. Chem. Soc.* **2010,** 132, (43), 15410-15417.
271. Szymanski, C.; Wu, C.; Hooper, J.; Salazar, M. A.; Perdomo, A.; Dukes, A.; McNeill, J., Single Molecule Nanoparticles of the Conjugated Polymer MEH−PPV, Preparation and Characterization by Near-Field Scanning Optical Microscopy. *J. Phys. Chem. B.* **2005,** 109, (18), 8543-8546.
272. Wu, C.; Szymanski, C.; Cain, Z.; McNeill, J., Conjugated Polymer Dots for Multiphoton Fluorescence Imaging. *J. Am. Chem. Soc.* **2007,** 129, (43), 12904-12905.
273. Sun, T.; Xie, Z., Conjugated Polymers and Polymer Dots for Cell Imaging. In *Fluorescent Materials for Cell Imaging*, Wu, F.-G., Ed. Springer Singapore: Singapore, 2020; pp 155-180.
274. Wu, C.; Jin, Y.; Schneider, T.; Burnham, D. R.; Smith, P. B.; Chiu, D. T., Ultrabright and Bioorthogonal Labeling of Cellular Targets Using Semiconducting Polymer Dots and Click Chemistry. *Angew. Chem. Int. Ed.* **2010,** 49, (49), 9436-9440.
275. Lin, Z.; Zhang, G.; Yang, W.; Qiu, B.; Chen, G., CEA fluorescence biosensor based on the FRET between polymer dots and Au nanoparticles. *Chem. Commun.* **2012,** 48, (79), 9918-9920.
276. Sun, F.; Wang, Z.; Feng, Y.; Cheng, Y.; Ju, H.; Quan, Y., Electrochemiluminescent resonance energy transfer of polymer dots for aptasensing. *Biosens. Bioelectron.* **2018,** 100, 28-34.
277. Bao, B.; Su, P.; Zhu, J.; Chen, J.; Xu, Y.; Gu, B.; Liu, Y.; Wang, L., Rapid aptasensor capable of simply detect tumor markers based on conjugated polyelectrolytes. *Talanta* **2018,** 190, 204-209.
278. Du, C.; Hu, Y.; Zhang, Q.; Guo, Z.; Ge, G.; Wang, S.; Zhai, C.; Zhu, M., Competition-derived FRET-switching cationic conjugated polymer-Ir(III) complex probe for thrombin detection. *Biosens. Bioelectron.* **2018,** 100, 132-138.
279. Gu, P.; Liu, X.; Tian, Y.; Zhang, L.; Huang, Y.; Su, S.; Feng, X.; Fan, Q.; Huang, W., A novel visible detection strategy for lysozyme based on gold nanoparticles and conjugated polymer brush. *Sens. Actuators B Chem.* **2017,** 246, 78-84.
280. Guo, L.; Hu, Y.; Zhang, Z.; Tang, Y., Universal fluorometric aptasensor platform based on water-soluble conjugated polymers/graphene oxide. *Anal. Bioanal. Chem.* **2018,** 410, (1), 287-295.
281. Liu, N.; Hui, N.; Davis, J. J.; Luo, X., Low Fouling Protein Detection in Complex Biological Media Supported by a Designed Multifunctional Peptide. *ACS Sens.* **2018,** 3, (6), 1210-1216.
282. Liu, X.; Hua, X.; Fan, Q.; Chao, J.; Su, S.; Huang, Y.-Q.; Wang, L.; Huang, W., Thioflavin T as an Efficient G-Quadruplex Inducer for the Highly Sensitive Detection of Thrombin Using a New Föster Resonance Energy Transfer System. *ACS Appl. Mater. Interfaces* **2015,** 7, (30), 16458-16465.
283. Nasirian, V.; Chabok, A.; Barati, A.; Rafienia, M.; Arabi, M. S.; Shamsipur, M., Ultrasensitive aflatoxin B1 assay based on FRET from aptamer labelled fluorescent polymer dots to silver nanoparticles labeled with complementary DNA. *Microchim. Acta* **2017,** 184, (12), 4655-4662.
284. Wang, C.; Tang, Y.; Guo, Y., Adenosine Deaminase Biosensor Combining Cationic Conjugated Polymer-Based FRET with Deoxyguanosine-Based Photoinduced Electron Transfer. *ACS Appl. Mater. Interfaces* **2014,** 6, (23), 21686-21691.

285. Zhang, Z.; Xia, X.; Xiang, X.; Huang, F.; Han, L., Conjugated cationic polymer-assisted amplified fluorescent biosensor for protein detection via terminal protection of small molecule-linked DNA and graphene oxide. *Sens. Actuators B: Chem.* **2017,** 249, 8-13.
286. Liu, Y.; Jiang, X.; Cao, W.; Sun, J.; Gao, F., Detection of thrombin based on fluorescence energy transfer between semiconducting polymer dots and bhq-labelled aptamers. *Sensors* **2018,** 18, (2), 589.